Identification of amino acid residues in the Ah receptor involved in ligand binding

Kenji Goryo [a], Ai Suzuki [b], Carlos A. Del Carpio [b], Kazuhiro Siizaki [c,1], Eisuke Kuriyama [a],
Yoshinori Mikami [a], Koshi Kinoshita [a], Ken-ichi Yasumoto [a], Agneta Rannug [d],
Akira Miyamoto [b], Yoshiaki Fujii-Kuriyama [a,2], Kazuhiro Sogawa [a,*]

[a] Department of Biomolecular Science, Graduate School of Life Sciences, Tohoku University, Sendai 980-8578, Japan
[b] Department of Materials Chemistry, Graduate School of Engineering, Tohoku University, Aoba-yama 6-6-11-1302, Sendai 980-8579, Japan
[c] Molecular and Cellular Toxicology Section, Environmental Health Sciences Division, National Institute for Environmental Studies, Onogawa, Tsukuba
305-8506, Japan
[d] Institute of Environmental Medicine, Karolinska Institutet, SE-171 77 Stockholm, Sweden

Received 19 December 2006
Available online 10 January 2007

Abstract

The Ah receptor (AhR) is a ligand-activated transcription factor. Five amino acids as candidate amino acids necessary for ligand binding within or near the ligand-binding domain were selected based on their evolutional conservation and their aromatic nature that could interact with xenobiotic ligands. These amino acids were changed to Ala, and the mutated AhRs were subjected to a test of their transactivation activity in HeLa cells. Mutation of Phe318 completely lost its activity whereas other mutations only weakly impaired activity. The Leu-substituted mutant, AhR(Phe318Leu), activated the luciferase activity to the level comparable to wild type in the cells treated with 3-methylcholanthrene (MC) but not at all with β-naphthoflavone (β-NF). Ligand-binding activity of mutants was examined with [³H]MC in vitro. AhR(Phe318Ala) could not bind to [³H]MC. [³H]MC bound by AhR(Phe318Leu) was competed with unlabeled MC but not with β-NF. A structural model of the ligand-binding domain was constructed.
© 2007 Elsevier Inc. All rights reserved.

Keywords: Ah receptor; Computer modeling; Ligand binding; PAS domain; Xenobiotics

Administration of xenobiotics such as 2,3,7,8-tetrachlorodibenzo-p-dioxin (TCDD), 3- methylcholanthrene (MC),

and β-naphthoflavone (β-NF) into experimental animals induces several drug-metabolizing enzymes such as CYP1A1 in the liver. These inducers act as ligands for the Ah receptor (AhR), and subsequently, the ligand-activated AhR activates transcription of genes encoding the enzymes [1]. Numerous environmental pollutants, agricultural chemicals, and drugs are known to serve as ligands for the AhR. Polyhalogenated aromatic hydrocarbons such as TCDD and coplanar polychlorinated biphenyls, polycyclic aromatic hydrocarbons such as 3-MC, benzo[a]pyrene and formylindolo[3,2-b]carbazoles, and flavonoids such as β-NF are representative potent ligands [1,2]. The most noticeable characteristic of the ligands is that they are organic molecules with planar aromatic rings. In resting cells, the AhR is associated with Hsp90 in the cytoplasm

as a soluble receptor. Owing to their lipophilic nature, it is presumed that ligands enter into cells by simple diffusion, and bind to the AhR. Ligand-induced conformation change of the AhR is believed to cause exposure of its nuclear localization signal and succeeding nuclear translocation of the liganded AhR. In the nucleus, the AhR forms a heterodimer with the Ah receptor nuclear translocator (Arnt), and then the heterodimer binds to a specific enhancer termed XRE (DRE or AhRE) localized in the upstream region of target genes [1]. The AhR and Arnt belong to the basic HLH–PAS domain protein family. Vertebrate PAS domains were generally composed of two imperfect repeated regions of about 110 amino acids named PAS-A and PAS-B domains. PAS and HLH domains serve as domains for dimerization with partner PAS proteins. In addition to the dimerization function, some PAS domains contain small organic compounds such as heme, probably for its sensing function [3]. The PAS-B domain of the AhR has the function of binding xenobiotic ligands [4]. The AhR homolog is also distributed in invertebrate species. Interestingly, recent studies demonstrate that *Drosophila* AhR (spineless) and *Caenorhabditis elegans* AhR (AhR-1) have no activity to bind foreign or endogenous chemicals as ligands. Although the protein has no ligand-binding activity, these AhRs heterodimerize with Arnt, binding to the DNA of which sequence is the same as XRE, and activating transcription [5,6].

In this study, we identified amino acids that play a key role in ligand binding of the AhR by several site-directed mutagenesis experiments. Furthermore, a three-dimensional model of the ligand-binding domain was constructed, which demonstrated good agreement with the results of the mutagenesis experiments.

Materials and methods

Construction of plasmids. pBOSFlag-mAhR-HA was constructed as follows. Oligonucleotides, 5′-CCACCGCCCATGGACTACAAAGACG ATGACGATAAAGGCATGGGCTGCA and 5′-GCCCATGCCTTTA TCGTCATCGTCTTTGTAGTCCATGGGCGGTGGAGCT for Flag peptide were inserted into the SacI and PstI site of pBluescript II. Full-length mouse AhR cDNA was inserted into the HindIII site of the generated plasmid. Using the plasmid as a template, a fragment of Flag-mAhR-HA was generated by PCR using primers, 5′-CCACCGCC CATGGACTACAAAGACGATGACGATAAAGGCATGGGCTGCA (forward) and 5′-CTCGAGCTAGGCGTAGGTCGGGCACGTCGAG GTCGACACACTCTGCACCTTGCTTAGGAATGCC (reverse), and the fragment was inserted into the XbaI site of the pEFBOS vector. Expression plasmids for mutated AhRs were produced by site-directed mutagenesis using PCR. Construction of XRE₄-tkLuc was described previously [7]. Chimeric plasmids for pFlag-mAhR-YFP were constructed as follows. A DNA fragment containing the Flag-AhR part of pBOSFlag-mAhR-HA was amplified by PCR, digested by BamHI and SalI and inserted into the NheI and XhoI sites of pEYFPN1 (Clonetech). The resultant plasmid was digested with EcoRI and BamHI, treated with Klenow fragment and self-ligated to make the sequence in-frame.

DNA transfection and Western blotting. HeLa cells were grown in MEM supplemented with 10% fetal bovine serum. DNA transfection into Hela cells (grown in a 60 mm dish) was carried out by the calcium phosphate method using 2 μg reporter plasmid XRE₄-tkLuc, 1 μg pBOSFlag-mAhR-HA, 1 μg pBOSmArnt, and 1 μg pBOSLacZ for internal control as

described [7]. Western blotting was performed using whole cell extracts from COS-7 cells transfected with pBOSFlag-mAhR-HA or its AhR mutants and a monoclonal anti-HA antibody (Roche, 12CA5). Because of low expression levels of the overexpressed proteins in HeLa cells, HEK293T cells were used to compare the expression levels of various mutants of the AhR, and it was found that they were relatively evenly expressed (data not shown).

Fluorescence observation of cells. CHO-K1 cells were provided by the Cell Resource Center for Biomedical Research, Institute of Development, Aging and Cancer, Tohoku University. Cells grown on the cover glass were transfected with 0.25 μg AhR–YFP fusion plasmids using FuGENE6 transfection reagent (Roche). After incubation for 40 h, cells were treated with MC or β-NF at a given concentration for 2 or 4 h, respectively. Imaging was performed with an Olympus BX50 fluorescence microscope equipped with a filter set (Olympus U-MYFPHQ) and an Olympus DP70 digital camera.

In vitro binding assay. Cytosolic extracts (1 mg protein/ml) from COS-7 cells transfected with expression plasmids for AhRs were prepared as described [8] and [³H]-labeled MC (1 μCi, 1.2 Ci/mmol, Moravek Biochemicals) was added to 450 μl of the extracts. The mixture was incubated at 4 °C for 2 h with or without unlabeled competitors, treated with dextran-coated charcoal and subjected to fractionation by 10–30% (v/v) glycerol gradient centrifugation at 50,000 rpm at 1 °C for 14 h.

Modeling the structure of PAS-B domain. The multiple alignment in the homology modeling procedure was performed based on the predicted and the observed secondary structures of the reference proteins, FixL [9], HERG [10], PHY3 [11,12], EC DOS [13], HIF-2α [14], and PAS kinase [15], while taking into consideration the sequence and structure conservation in their families. A homology model of the mAhR PAS-B domain was generated by means of the modeling module in Insight 2000 (Accelrys Inc.). The docking process was performed using the docking module of the Cerius² system (Accelrys Inc.).

Results

Transactivation activity of mutated AhR

Candidate amino acids for ligand recognition and binding were selected on the basis of the following two assumptions. (1) Amino acids are conserved among vertebrate species whose AhRs exhibit ligand-binding activity, but are not conserved in the *Drosophila* and *C. elegans* AhRs that are deficient in binding activity. (2) Interactions between ligands and amino acids include the stacking force between aromatic side chains and aromatic rings of ligands because all ligands have hydrophobic aromatic rings. There were a number of amino acids that satisfied the first criterion. Accordingly, the second criterion was placed on the amino acids. Selection of amino acids satisfying the two criteria revealed five aromatic amino acids within and near the PAS-B domain as shown in Fig. 1A. The amino acids were mutated to Ala, and the transactivation activity of the corresponding mutated AhR was assayed. As shown in Fig. 1B, activity decreased to the basal level in the presence of MC by mutation of Phe318 to Ala. This loss of activity was also seen with other inducers including TCDD and β-NF. Other mutations caused a slight decrease in the transactivation activity. The Phe318 was changed to other amino acids as shown in Fig. 1C, and the transactivation activity of the mutated AhRs was assayed. Substitution to aromatic amino acids, Tyr or Trp, showed an inducible luciferase activity by the stimulus of MC and β-NF,
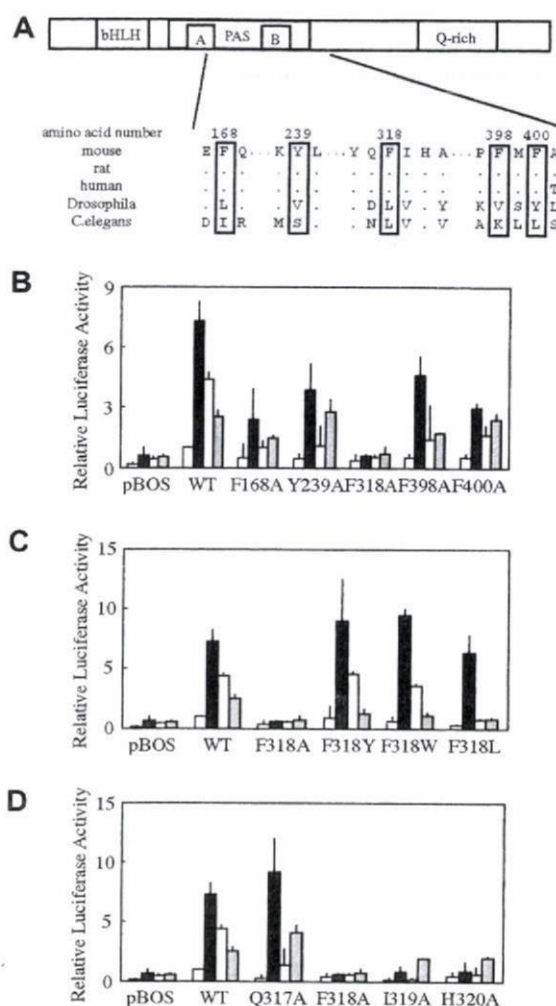
Fig. 1. Transactivation activity of the AhR and its mutants. (A) Alignment of the PAS-B sequences of vertebrate and invertebrate AhR. Structure of the mouse AhR is schematically shown above. Aromatic amino acid residues that were conserved within and around the PAS-B domain of mouse, human, and rat AhRs and that were not conserved in the domain of *Drosophila* and *C. elegans* AhRs were boxed. Dots indicate the same amino acids as those of the mouse AhR. (B) Transactivation activity of the AhRs with mutation of selected amino acids shown in (A). Selected aromatic amino acids were mutated to Ala, and cotransfected into HeLa cells with a reporter plasmid. Four hours after transfection, MC (1 μM), β-NF (0.5 μM), or TCDD (10 nM) were added to the culture medium and cells were further incubated for 40 h. Luciferase activity driven by the AhRs is shown. The values represent means ± SD of at least three separate determinations, and were normalized using the value(s) of wild type AhR treated with DMSO. Open bars, DMSO (vehicle); filled bars, MC; light gray bars, β-NF; dark gray bars, TCDD. (C,D) Transactivation activity of the AhRs with mutations of Phe318 to Ala, Tyr, Trp, and Leu, and transactivation activity of the AhRs with mutation of amino acids neighboring Phe318. Experimental procedures are shown in (B).

probably because the aromatic nature of the side chain was preserved, although induction by TCDD was weak. Mutation to Leu showed a luciferase activity in response to MC with an induction ratio similar to that of wild type, although induced activity was somewhat lower than that

of wild type. Interestingly, this mutant exhibited no induction of luciferase activity by the addition of β-NF or TCDD, indicating that this mutation caused a ligand-binding specificity different from the wild type and suggesting that Phe318 may have contact with ligands. Three amino acid residues neighboring Phe318 were changed to Ala. The mutation of Gln317 had no effect on activity although induction by β-NF was weak (Fig. 1D). The mutation of Ile319 or His320 resulted in complete loss of activity, suggesting that these two amino acids also play an important role for ligand binding.

Nuclear translocation of AhRs in response to inducers

Chimeric proteins of mutated AhRs fused to YFP were expressed in CHO-K1 cells, and subcellular localization of the chimeric proteins was observed. These chimeric proteins were evenly expressed and showed transactivation activity similar to the AhR without YFP tag (data not shown). Fluorescence from the YFP moiety of the wild-type AhR fusion protein was diffused over the cell, and treatment of cells with MC caused accumulation of the signal in the nucleus as shown in Fig. 2. Approximately 50% of the fluorescent cells showed nuclear localization at the maximal concentration of MC. The nuclear accumulation was accomplished within 2 h and dependent on the concentration of MC. Nuclear translocation was also observed by the addition of β-NF, although the rate of the translocation was slow, and 4 h was required for completion. The reason is not clear as to why nuclear localization of expressed AhR–YFP did not occur in all fluorescent cells even at high concentrations of inducers. Nuclear localization of mutant AhR(Phe318Ala) was similarly examined. When neither MC nor β-NF was added, nuclear accumulation of the mutant did not occur. Mutant AhR(Phe318Leu) was translocated into the nucleus by the addition of MC similar to the level of the wild type. However, the mutant remained in the cytosol with the addition of β-NF, in accordance with the result of transactivation activity of the mutant. Taken together, these results strongly suggest that stimulus-dependent nuclear localization of mutated AhRs is the causal event for their transactivation activity.

Ligand-binding activity of mutated AhRs

In vitro binding activity of mutated AhRs to [³H]-labeled MC was examined using cytosolic extracts of COS-7 cells transfected with expression plasmids for the AhRs. A clear peak at around the 9S position of the [³H]MC-AhR complex appeared in the glycerol gradient as shown in Fig. 3A. This binding of the radioactive ligand was competed out with 22 times the molar excess of unlabeled MC or β-NF. A similar binding signal was also observed when cytosol containing AhR(Phe318Leu) was used. This signal was competed with unlabeled MC. However, unlabeled β-NF could not compete with the [³H]MC bound to the mutated AhR, reflecting the results of transactivation and
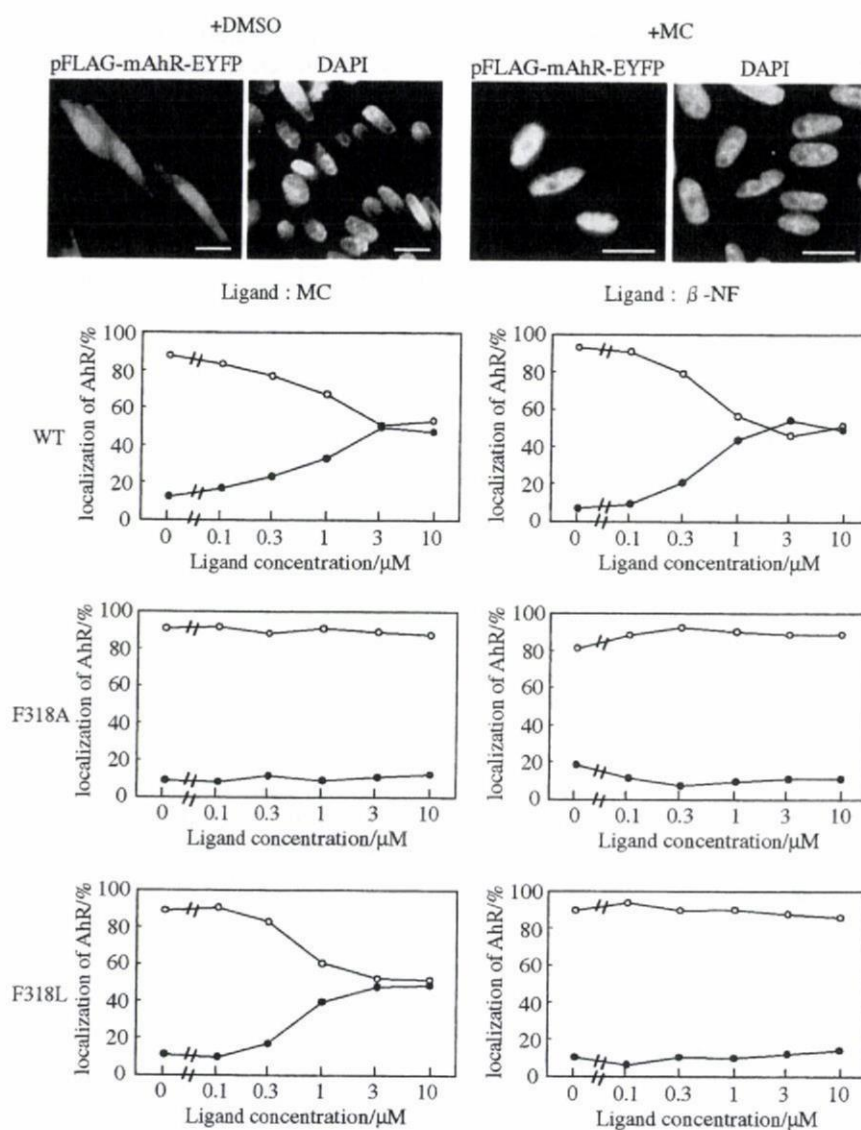
Fig. 2. Nuclear translocation of the AhR and its mutants. CHO-K1 cells were transfected with AhR–YFP-fusion plasmids, and treated with inducers for 2 h (MC) or 4 h (β-NF) before fixation in 4% paraformaldehyde. The fixed cells were counterstained with DAPI. Typical images of fluorescent cells after treatment with DMSO (vehicle) and MC are shown above. Scale bars, 20 μm. Approximately 300 cells were randomly selected, and percentages of cells with only nuclear localization (shown by closed circles) and cells with both nuclear and cytosolic localization (shown by open circles) of the chimeric protein are shown.

nuclear translocation experiments. When cytosol fraction containing expressed AhR(Phe318Ala) was used, no signal of ligand binding was detected. The mutated AhRs were evenly expressed in COS-7 cells as shown in Fig. 3B.

Modeling the AhR ligand-binding domain

Since the three-dimensional (3D) structure of AhR has not been elucidated so far, and previously reported 3D models of the ligand-binding domain have failed to identify Phe318 as a ligand-recognition amino acid [16], we concentrated on the active site of AhR, and obtained a 3D model for it using comparative modeling techniques. A combined

FASTA and PSI-BLAST search of the protein data bank (PDB) [17] reveals a high number of matches between mouse AhR PAS-B and other PAS proteins, including HLF (HIF-2α), several histidine kinases, and other light receptors as well as sensor proteins (oxygen/redox sensors) and ion channels (data not shown). Sequences such as HLF, PHY3, HERG, FixL, EC Dos, and PAS kinase were found that were based on a moderate sequence similarity, characterized by E values of less than 10^{-3}. Fig. 4A illustrates the multiple sequence alignment of AhR PAS-B with these sequences. A further alignment of the secondary structure predicted for AhR PAS-B and the secondary structures for the 3D structures extracted from PDB
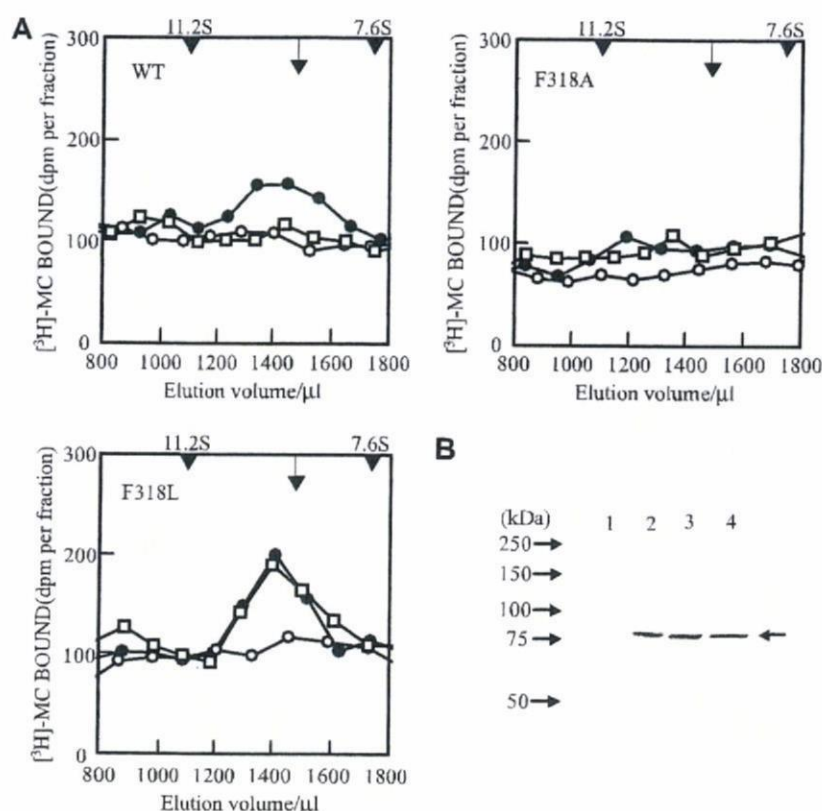
Fig. 3. Ligand-binding activity of the AhR and its mutants. (A) Binding of mutant AhRs to [³H]-labeled MC. AhRs were expressed in COS-7 cells and cytosolic extracts were prepared. Glycerol gradient centrifugation was performed as described under Materials and methods. Fractions (about 100 μl) were collected and radioactivity was counted on a liquid scintillation counter. Catalase (11.2S) and fibrinogen (7.6S) were used as size markers. Arrows show the position of 9S. Filled circle, [³H]MC with DMSO; open circle, [³H]MC with unlabeled MC; open square, [³H]MC with unlabeled β-NF. (B) Expression of mutant AhRs. Western blotting analysis using 20 μg of cell extracts was performed by the ECL plus Western blotting detection system kit. Lane 1, whole cell extracts without transfection; lanes 2–4, cytosolic extracts of cells transfected with expression plasmid for AhR, AhR(Phe318Ala), and AhR(Phe318Leu), respectively. An arrow shows the bands of the AhR.

indicate that the fold of HLF is the optimal template on which to model AhR PAS-B (Fig. 4B). The threading process of the AhR sequence into the template was performed using Swiss PDB viewer (spdbv) software. The structure was further minimized using the GROMOS force field embedded in spdbv to optimize the position of the lateral chains of the amino acids constituting the receptor.

Assisted by the docking module in Cerius², we first mapped plausible ligand-binding pockets for the model of AhR PAS-B. A unique deep cavity was recognized by the system, the boundaries of which are constituted by the amino acids in Table 1. The model was then used to dock three ligand molecules, MC, β-NF, and TCDD. The docking process was also performed using the Cerius² software. Orientations for the ligands within the binding pocket ranked as the highest by the docking software were further minimized so as to obtain reliable 3D structures for the receptor–ligand complexes. Amino acids in contact with the ligand are identified by computing the fraction of SASA (solvent accessible surface area) buried by each of the amino acids on the ligand. We performed this calculation for β-NF, and Table 1 illustrates the decrement in

SASA of β-NF when docked to the cavity of the model of AhR by each of the amino acids composing the cavity. The SASA is computed using Richards' algorithm [18], and a radius for the solvent molecule (water) of 1.4 Å. The buried SASA is calculated as the difference of the SASA of β-NF at the isolated state minus the SASA of β-NF when it is in contact with each of the amino acids listed in Table 1. Docking models of the complex of AhR with TCDD, MC or β-NF, show their extensive contact with Phe318, Ile319, and His320 (Fig. 4C). Extensive hydrophobic interaction can also be observed with Ala328, Met342, Leu347, and Leu348. Two lysine residues (Lys284 and Lys286) suggest the formation of hydrogen bonds with the oxygens on the aromatic rings of β-NF.

Discussion

From the results shown in Fig. 1, it is suggested that Phe318 plays a critical role in ligand binding to AhR. The importance of this amino acid is also demonstrated by the complex model of AhR PAS-B that we built by comparative modeling and docking simulations. The decrement
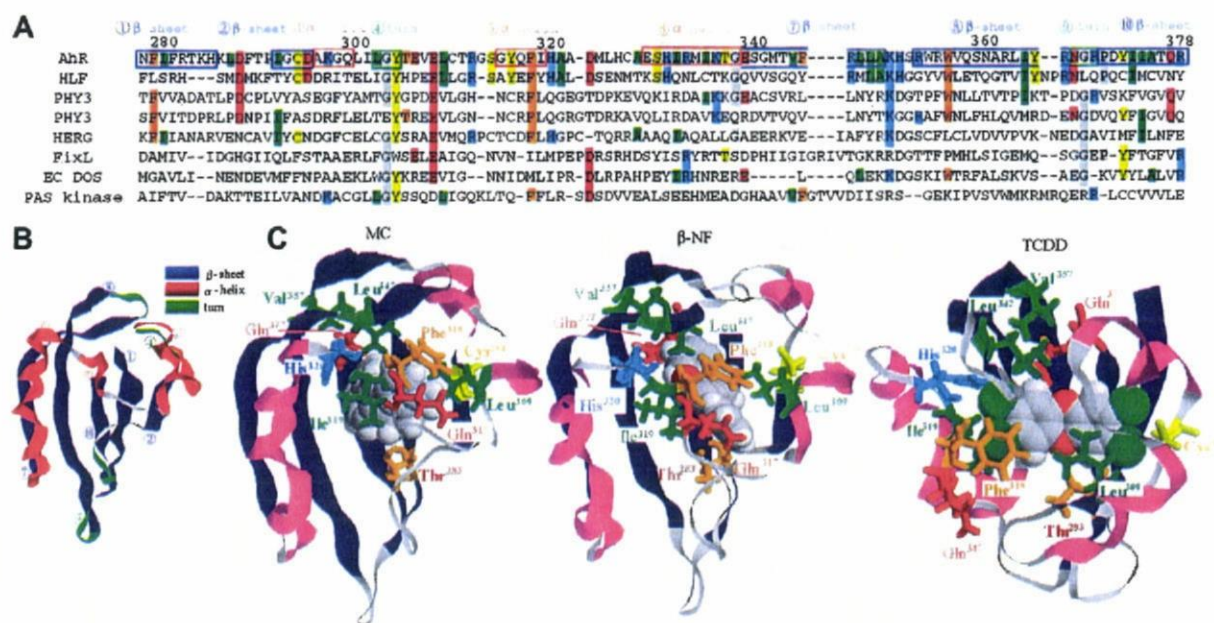
Fig. 4. Model of the AhR PAS-B domain and contacts between ligands and amino acid residues in the binding pocket. (A) Sequence alignment of AhR-related sequences. Sequences of Mouse AhR, human HLF (HIF-2α), PHY3 from *Chlamydomonas reinhardtii* (upper sequence) and *Adiantum capillus-veneris* (lower sequence), human HERG, *Bradyrhizobium japonicum* FixL, *Escherichia coli* EC DOS and human PAS kinase were aligned. Secondary structure regions are shown above the sequences. (B) Ribbon-style drawing of the AhR PAS-B domain. Numbers show the secondary structure regions as shown in (A). (C) Model of MC, β-NF, and TCDD in the binding site of AhR PAS-B domain. Secondary structure elements are colored blue (strands) and red (helices).

Table 1
Calculated buried SASA of β-NF by amino acids in the binding region of AhR

Amino acid	Difference in SASA (in Å^2) for β-NF
THR283	0.07
LYS284	73.37
LYS286	49.73
CYS294	0.07
GLN299	72.54
GLY303	47.77
TYR304	29.22
LEU309	0.07
CYS310	27.07
GLY315	46.93
GLN317	0.07
PHE318	84.37
ILE319	77.81
HIS320	60.62
ALA328	81.26
SER330	43.35
MET342	73.18
LEU347	88.59
LEU348	87.90
ALA349	42.20
VAL357	37.66
SER359	61.20
ALA375	0.00
GLN377	41.40

in the SASA of β-NF due to contact with Phe318 is large (about 84 Å^2, Table 1), suggesting that extensive interaction exists between the residue and the ligand. Mutation of Phe318 by Leu completely eliminated responsiveness of the mutant towards β-NF, although responsiveness to MC remained unchanged. Binding experiments using [^{3}H]MC corroborate the geometry of our modeled complex, since the location of Phe318 at the ligand-binding surface of the receptor plays a key role in ligand-binding specificity. This is clearly shown by the mutations performed on Phe318 that caused changes in the binding activity of the receptor. Moreover, two amino acids, Ile319 and His320, neighboring Phe318, were both found to play an essential role in the binding activity of the receptor. Although contact surface areas of these amino acids with the docked ligands are less than that of Phe318, their relevance in the binding affinity of the receptor cannot be neglected. In fact, Ile319 has been reported to be important in avian AhRs [19]. The Ile residue (Ile324 corresponding to Ile319 in the mouse AhR) of the chicken AhR that showed high affinity towards TCDD was changed to Val in tern AhR that exhibited low TCDD-binding activity. As shown in Fig. 1D, a large decrement in the activity of the receptor was observed when they were mutated to Ala. Therefore, the importance of these two amino acids in the binding of the ligands can be rationalized in terms of their bulky lateral chains and polar characteristics. The imidazole group in His confers it a polar property absent in Ala while Ile has a larger chain and is more strongly hydrophobic. Thus, mutations of these amino acids have strong repercussions in the activity of the receptor. Ala375, whose allelic mutation was demonstrated to be

responsible for the different ligand-binding affinity between C57BL/6 and DBA/2 mouse strains [8] was also exposed into the ligand-binding pocket, although it does not appear to be in direct contact with β-NF in the model. Further mutagenesis studies are necessary to confirm the amino acids composing ligand-binding domain of the AhR.

Acknowledgments

References

[1] J. Mimura, Y. Fujii-Kuriyama, Molecular mechanisms of AhR functions in the regulation of cytochrome P450 genes, Biochem. Biophys. Res. Commun. 338 (2005) 311–317.

[2] L. Bergander, N. Wahlstrom, T. Alsberg, J. Bergman, A. Rannug, U. Rannug, Characterization of in vitro metabolites of the aryl hydrocarbon receptor ligand 6-formylindolo[3,2-b]carbazole by liquid chromatography-mass spectrometry and NMR, Drug Metab. Dispos. 31 (2003) 233–241.

[3] E.M. Dioum, J. Rutter, J.R. Tuckerman, G. Gonzalez, M.A. Gilles-Gonzalez, S.L. Mcknight, NPAS2: a gas-responsive transcription factor, Science 298 (2002) 2385–2387.

[4] K.M. Dolwick, H.I. Swanson, C.A. Bradfield, In vitro analysis of Ah receptor domains involved in ligand-activated DNA recognition, Proc. Natl. Acad. Sci. USA 90 (1993) 8566–8570.

[5] J.A. Powell-Coffman, C.A. Bradfield, W.B. Wood, Caenorhabditis elegans orthologs of the aryl hydrocarbon receptor and its heterodimerization partner the aryl hydrocarbon receptor nuclear translocator, Proc. Natl. Acad. Sci. USA 95 (1998) 2844–2849.

[6] R.B. Emmons, D. Duncan, P.A. Estes, P. Kiefel, J.T. Mosher, M. Sonnenfeld, M.P. Ward, I. Duncan, S.T. Crews, The spineless-aristapedia and tango bHLH-PAS proteins interact to control antennal and tarsal development in Drosophila, Development 126 (1999) 3937–3945.

[7] J. Mimura, M. Ema, K. Sogawa, Y. Fujii-Kuriyama, Identification of a novel mechanism of regulation of Ah (dioxin) receptor function, Genes Dev. 13 (1999) 20–25.

[8] M. Ema, N. Ohe, M. Suzuki, J. Mimura, K. Sogawa, S. Ikawa, Y. Fujii-Kuriyama, Dioxin binding activities of polymorphic forms of mouse and human arylhydrocarbon receptors, J. Biol. Chem. 269 (1994) 27337–27343.

[9] W. Gong, B. Hao, S.S. Mansy, G. Gonzalez, M. Gilles-Gonzalez, M.K. Chan, Structure of a biological oxygen sensor: a new mechanism for heme-driven signal transduction, Proc. Natl. Acad. Sci. USA 95 (1998) 15177–15182.

[10] J.H.M. Cabral, A. Lee, S.L. Cohen, B.T. Chait, M. Li, R. Mackinnon, Crystal structure and functional analysis of the HERG potassium channel N terminus: a eukaryotic PAS domain, Cell 95 (1998) 649–655.

[11] S. Crosson, K. Moffat, Photoexcited structure of a plant photoreceptor domain reveals a light-driven molecular switch, Plant Cell 14 (2002) 1067–1075.

[12] T. Kinoshita, M. Doi, N. Suetsugu, T. Kagawa, M. Wada, K. Shimazaki, Phot1 and phot2 mediate blue light regulation of stomatal opening, Nature 414 (2001) 656–660.

[13] H. Kurokawa, D.S. Lee, M. Watanabe, I. Sagami, B. Mikami, C.S. Raman, T. Shimizu, A redox-controlled molecular switch revealed by the crystal structure of a bacterial heme PAS sensor, J. Biol. Chem. 279 (2004) 20186–201893.

[14] P.J. Erbel, P.B. Card, O. Karakuzu, R.K. Bruick, K.H. Gardner, Structural basis for PAS domain heterodimerization in the basic helix–loop–helix-PAS transcription factor hypoxia-inducible factor, Proc. Natl. Acad. Sci. USA 100 (2003) 15504–15509.

[15] J. Rutter, C.H. Michnoff, S.M. Harper, K.H. Gardner, S.L. McKnight, PAS kinase: an evolutionarily conserved PAS domain-regulated serine/threonine kinase, Proc. Natl. Acad. Sci. USA 98 (2001) 8991–8996.

[16] M. Procopio, A. Lahm, A. Tramontano, L. Bonati, D. Pitea, A model for recognition of polychlorinated dibenzo-p-dioxins by the aryl hydrocarbon receptor, Eur. J. Biochem. 269 (2002) 13–18.

[17] H.M. Berman, J. Westbrook, Z. Feng, G. Gilliland, T.N. Bhat, H. Weissig, I.N. Shindyalov, P.E. Bourne, The protein data bank, Nucleic Acids Res. 28 (2000) 235–242.

[18] B. Lee, F.M. Richards, Interaction of protein structures: estimation of static accessibility, J. Mol. Biol. 55 (1971) 379–400.

[19] S.I. Karchner, D.G. Franks, S.W. Kennedy, M.E. Hahn, The molecular basis for differential dioxin sensitivity in birds: role of the aryl hydrocarbon receptor, Proc. Natl. Acad. Sci. USA 103 (2006) 6252–6257.

Quantitative analysis of benzo[a]pyrene biotransformation and adduct formation in Ahr knockout mice

Carlos Sagredo [a], Steinar Øvrebø [a], Aage Haugen [a], Yoshiaki Fujii-Kuriyama [b], Rita Bæra [a], Ingrid V. Botnen [a], Steen Mollerup [a],*

[a] *Section for Toxicology, National Institute of Occupational Health, P.O. Box 8149 Dep., N-0033 Oslo, Norway*
[b] *TARA Center, University of Tsukuba, Tsukuba, Japan*

Abstract

Benzo[a]pyrene (BP) is an ubiquitous environmental pollutant with potent mutagenic and carcinogenic properties. The Ah receptor (Ahr) is involved in the metabolic activation of BP and is therefore important in the induction of chemical carcinogenesis. In this study, the relationship between Ahr genotype and biotransformation of BP in internal organs was investigated in Ahr (+/+), Ahr (+/−) and Ahr (−/−) mice. The mice were treated with BP (100 mg/kg) by gavage. Gene expression was measured after 24 h by real-time RT-PCR and showed induction of Cyp1a1 in liver and lung, and Cyp1b1 in lung in both Ahr (+/+) and Ahr (+/−). No induction of the Cyp genes was observed in the Ahr (−/−). There was a significant basal expression of Cyp1b1 in the liver of all genotypes, and this expression was independent of the BP exposure. Analyzed by HPLC-fluorescence, there were increased levels of protein and DNA adducts, metabolites, conjugates and unmetabolized BP in the internal organs of Ahr (−/−) as compared to Ahr (+/+) and Ahr (+/−) mice. This may be partly explained by a delayed bioactivation of BP in the Ahr deficient mice. The BP metabolism observed in the Ahr (−/−) mice is also evidence of an Ahr independent biotransformation of BP.
© 2006 Elsevier Ireland Ltd. All rights reserved.

Keywords: Aryl hydrocarbon receptor; Knockout mice; Benzo[a]pyrene; Benzo[a]pyrene adducts; Benzo[a]pyrene metabolites; Cytochrome P450

1. Introduction

Polycyclic aromatic hydrocarbons (PAHs) constitute a large class of compounds formed during incomplete combustion of organic matter and fossil fuels in industrial processes, automobile exhaust, cigarette smoke and charbroiled food (IARC Monographs, 1983a,b). Exposure to PAHs is high in certain occupational environments. Several of the PAH congeners are classified as carcinogens. Benzo[a]pyrene (BP) is a well-studied member of the PAH family and has served as a model for the biotransformation and carcinogenic effects of PAHs (Conney, 1982; Dipple, 1995; Harvey and Geacintov, 1988; Hogan et al., 1981; Stowers and Anderson, 1985). BP and other PAHs are primarily activated by P450 enzymes regulated by the aryl hydrocarbon receptor (Ahr) pathway (Whitlock, 1999). The Ahr also plays an important role in the regulation of cell growth and differentiation. The discovery of the Ahr originated from studies with Ah responsive/non-responsive mouse models (Nebert, 1989). The importance of the Ahr in the activation of PAH has then led to several Ahr and cytochrome P450 knockout mouse models (Kondraganti et al., 2003; McFadyen et al., 2003; Nakatsuru et

* Corresponding author. Tel.: +47 23 19 52 97;
fax: +47 23 19 52 03.
  E-mail address: steen.mollerup@stami.no (S. Mollerup).

al., 2004; Shimizu et al., 2000; Uno et al., 2004, 2006).

BP acts as a ligand and binds to the Ahr in the cytoplasm. The liganded Ahr is then translocated to the nucleus where it forms a heterodimer with the Ahr-nuclear translocator (Arnt). The Ahr/Arnt heterodimer recognize and binds to xenobiotic responsive element (XRE) sequences located in the promoter region of several genes such as cytochrome P450 (Cyp)1a1, Cyp1a2, Cyp1b1, glutathione S-transferases (Gst), and UDP-glucoronosyl-transferases (Ugt) (Nebert et al., 2000; Whitlock, 1999). The binding results in transcriptional activation of the genes and induction of phases I and II metabolizing enzymes as well as phase III transporter proteins (Klaassen, 2002; Xu et al., 2005). The

encoded cytochrome P450 enzymes will then transform PAH to hydroxyl containing metabolites that are rapidly conjugated to glucoronides and sulphates by phase II enzymes. The bioactivation of BP goes through reactive intermediates, like epoxides, that may produce DNA and protein adducts (Fig. 1). The formation of covalent DNA adducts is an important first step in the initiation of PAH induced carcinogenesis (Hogan et al., 1981; Stowers and Anderson, 1985), and it has been suggested that increased adduct levels may be predictive of cancer risk (Veglia et al., 2003).

Shimizu et al. (2000) found that BP carcinogenicity was lost in mice lacking the Ahr. The mice received topical application and subcutaneous injection of the PAH, and only the Ahr (+/+) and Ahr (+/−) mice developed
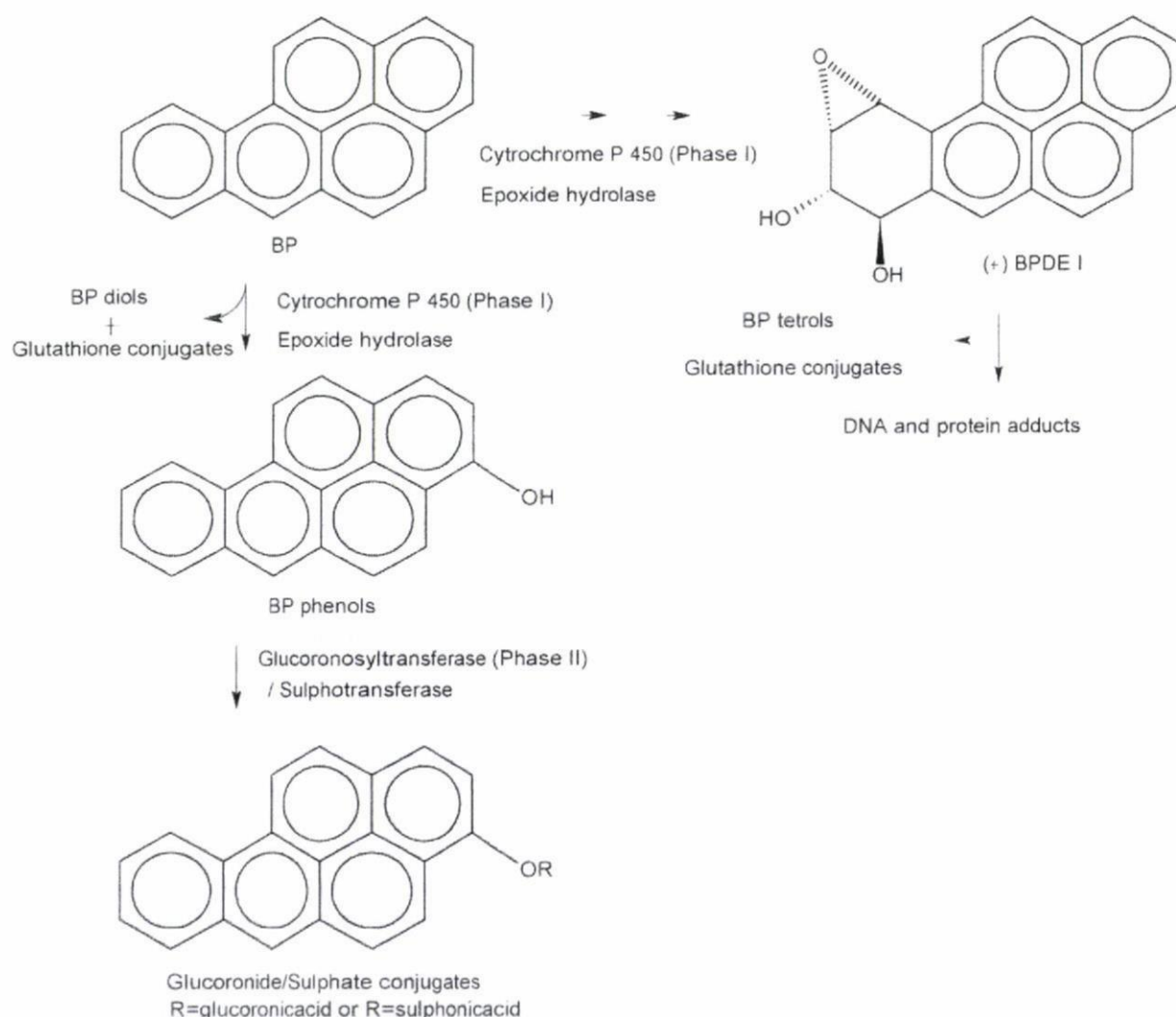

Fig. 1. Metabolism of BP by the cytochrome P450 (phase I) that initially transform BP to hydroxyl containing metabolites. Reactive epoxides are rapidly hydrolysed by epoxide hydrolase or conjugated by glutathione transferase. The horizontal reaction illustrates the formation of the ultimate carcinogenic metabolite, the 7,8-diol-9,10-epoxide (BPDE I) that may form DNA and protein adducts. The vertical reaction illustrates the detoxifying pathway of metabolites by phase II conjugation.

tumors. Kondraganti et al. (2003) found that total hepatic BP-DNA adduct levels were almost equal in Ahr (−/−) and Ahr (+/+) mice after a single i.p. dose of BP. In the knockout studies by Uno et al. (2004, 2006), it was shown that BP-DNA adducts and genotoxicity increased in the absence of the Cyp 1a1 and Cyp 1b1 genes.

To gain further insight in the role of the Ahr in the metabolic activation and detoxication of PAH, we have studied the relationship between Ahr genotype and bioactivation and biotransformation of BP in internal organs. In contrast to previous studies we have treated the animals with a single dose of BP by gavage. In the present report, we have quantitated protein and DNA adducts and metabolites. By the use of a highly specific HPLC-fluorescence method, we find increased levels of protein and DNA adducts, metabolites and unmetabolized BP in the Ahr (−/−) as compared to Ahr (+/+) mice. Gene expression has been measured by quantitative real-time RT-PCR.

2. Materials and methods

2.1. Chemicals and standards

(±)-Benzo[a]pyrene-r-7,t-8,t-9,c-10-tetrahydrotetrol (BP-tetrol I-1), (±)-benzo[a]pyrene-r-7,t-8,t-9,10-tetrahydrotetrol (BP-tetrol I-2), (±)-benzo[a]pyrene-r-7,t-8,c-9,t-10-tetrahydrotetrol (BP-tetrol II-1), (±)-benzo[a]pyrene-r-7,t-8,c-9,c-10-tetrahydrotetrol (BP-tetrol II-2), benzo[a]pyrene-4,5-dihydrodiol, benzo[a]pyrene-7,8-dihydrodiol, benzo[a]-pyrene-9,10-dihydrodiol, benzo[a]pyrene-3-phenol and benzo[a]pyrene-9-phenol were purchased from the National Cancer Institute (NCI), Chemical Carcinogen Repository (Midwest Research Institute, Kansas City, MO, USA). The two remaining tetrols, BP-tetrol III-1 and BP-tetrol III-2 were prepared in our laboratory as described earlier (Sagredo et al., 2006). Benzo[a]pyrene was purchased from Sigma (St. Louis, MO, USA). HPLC grade methanol was obtained from Fluka (Buchs, Switzerland). Water was obtained from a Milli-Q ultrapure water purification system (Milipore, Bedford, MA, USA). Benzo[a]pyrene glucoronide and sulphate conjugates were prepared in our laboratory.

2.2. Animals and treatment

The Ahr heterozygote model (C57BL6) has been described previously (Shimizu et al., 2000). The animals were acclimatized after arrival in a germ free facility using air-filtered controlled environment. The Ahr (+/−) were interbred to generate Ahr (+/+), Ahr (+/−) and Ahr (−/−) mice. Genotyping was carried out as described previously (Shimizu et al., 2000). The formation of the knockout offspring did not follow the Mendelian law, since repeatedly only about 10–15% of the offspring had the Ahr (−/−) genotype. Real-time RT-PCR measurement of AHR expression was carried out on lung tissue samples at the end of the experiments to verify genotypes. There were no observed differences in growth rate and appearance between the different genotypes. The animals were fed standard diet (B&K Universal A/S, Norway) and water ad libitum. BP was solubilized in corn oil (10 mg/ml) and the animals were treated with a single dose of BP (100 mg/kg) by gavage. Three females and 3 males of each genotype were included, in total 18 animals. The control group of three animals, one of each genotype, received pure corn oil. After 24 h, the animals were sacrificed and lung, liver, spleen, kidney and heart were removed and blood samples collected. The experiments were repeated with similar result (data not shown). All animal handling and experimental procedures were conducted in conformity with laws and regulations controlling experiments on live animals in Norway and the European Convention for the Protection of Vertebrate Animals used in Experimental and Other Scientific Purposes.

2.3. Protein and DNA isolation

Harvested organs were homogenized in a phosphate buffer solution using a mixer mill followed by a brief centrifugation. The pellet was used for DNA isolation (liver) and the supernatant for protein and metabolite quantification. Protein concentrations were determined by the Lowry method (Lowry et al., 1951). Blood from the animals was collected with Na-heparin, and plasma separated by centrifugation at $1200 \times g$ for 15 min. The plasma and the supernatant were withdrawn and proteins were precipitated with the addition of two volumes of cold acetone. Samples were left for 30 min followed by centrifugation at $1200 \times g$. The precipitated proteins were washed twice with 4 ml acetone:ethylacetate (1:1) to remove unbound BP metabolites. The washing fractions were pooled and stored for HPLC analysis. The precipitate was air dried at room temperature and solubilized in 900 μl of 10 mM Tris–HCl/1 mM EDTA pH 8.0. DNA was isolated as described by Beach and Gupta (1992). DNA concentration was quantitated spectrophotometrically and by fluorescence measurements with a Hoechst 33258 instrument.

2.4. Adduct purification

BP-protein and DNA adducts were measured as released BP-tetrols after acid hydrolysis. The ultimate carcinogenic diolepoxide, BPDE-I, gives rise to the two tetrols BP-tetrol-I-1 and BP-tetrol-I-2. The less carcinogenic diolepoxide, BPDE-II, gives rise to the two tetrols BP-tetrol-II-1 and BP-tetrol-II-2. In addition, two BP-tetrols were detected after DNA and protein hydrolysis, originating from the non-bay region diolepoxide, BPDE III (Sagredo et al., 2006).

The 900 μl protein solution was added 100 μl of 1 M HCl, and this solution was incubated at 70 °C for 3 h. Water and methanol were added to a final volume of 5 ml with 10% methanol. This solution was applied to preconditioned Sep-Pak C$_{18}$ cartridges (Millipore, Milford, MA) followed by 10 ml washing with water and the tetrols were eluted with 5 ml methanol. The eluate was evaporated at 45 °C under a nitro-

gen stream and resolubilized in 500 μl of 10% methanol. The samples were stored at −20 °C.

2.5. HPLC-fluorescence quantitation

The analysis was performed on an Agilent 1100 LC system using a Hypersil ODS, 5 μm, 3.9 mm × 150 mm column (Agilent) equipped with an Agilent 1100 fluorescence detector. The column temperature was 40 °C and the flow rate was set at 1 ml/min. The injection volume was typically 20 μl and the samples were separated by a linear gradient of water and methanol by increasing the methanol content from 30% to 100% in 40 min. The excitation and emission wavelengths were 341 and 381 nm, respectively. The benzo[a]pyrene glucoronide and sulphate conjugates were analyzed directly without any previous hydrolysis. Separation was achieved using a 10 mM amoniumphosphate buffer (pH 6) at a flow rate of 0.8 ml/min. The linear gradient of buffer and methanol was increased from 20% to 98% methanol in 55 min.

2.6. Gene expression

Gene expression measurements were carried out by quantitative real-time RT-PCR on an ABI PRISM 7900 (Applied Biosystems) as described previously (Berge et al., 2004). In brief, total RNA was reverse transcribed by the aid of random primers. Primers for β-actin (Actb), Cyp1a1 and Cyp1b1 were as in Berge et al. (2004). Primer for Ahr were designed by the PrimerExpress 2.0.0 software (Applied Biosystems) and the sequences were: Ahr upper: 5′-CAG TCC AAT GCA CGC TTG ATT-3′, Ahr lower: 5′-ACA GCC TCT CCG GTA GCA AA-3′ (146 bp). The amount of target cDNA in each sample was established by determining a fractional PCR threshold cycle number (C_t-value). Specific gene expression levels were normalized to the expression of β-actin and calculated by the formula: $2^{-(C_t\text{gene}-C_t\beta\text{-actin})}$.

2.7. Statistical analysis

For the analysis of gene expression, protein adducts and metabolites, means were compared by the independent-samples t-test. Due to significant variations in standard deviation Welch correction was applied.

3. Result

In animals exposed to BP, real-time RT-PCR analysis showed induction of Cyp1a1 in liver and lung in both Ahr (+/+) and Ahr (+/−) but no induction in the Ahr (−/−) (Fig. 2A). There was also an induction of Cyp1b1

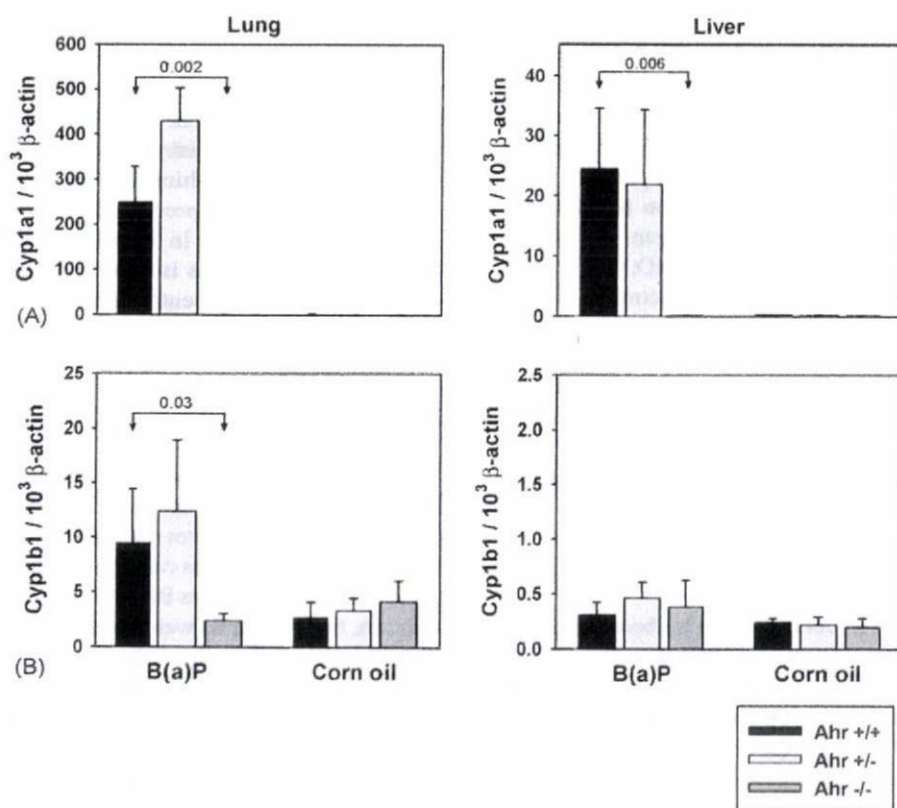Fig. 2. (A) Cyp1a1 and (B) Cyp1b1 levels in lung and liver tissues were measured by real-time RT-PCR and normalized to the expression of β-actin. Mice were given a single oral dose with BP (100 mg/kg) in corn oil (n = 6) for 24 h and pure corn oil for the control group (n = 3). Means were compared by the independent samples t-test with Welch correction.
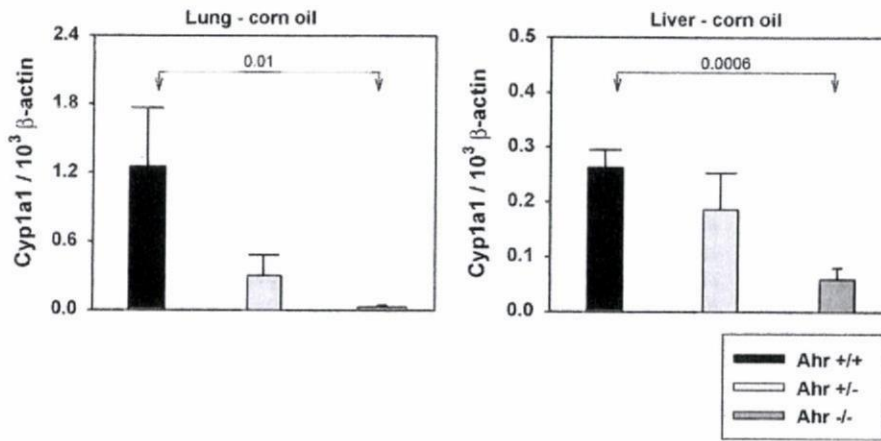
Fig. 3. Basal expression of Cyp1a1 in lung and liver of Ahr (+/+), Ahr (+/−) and Ahr (−/−) mice ($n = 3$) exposed to corn oil. Cyp1a1 expression was normalized to the expression of β-actin. Means were compared by the independent samples t-test with Welch correction.

in the lung of both Ahr (+/+) and Ahr (+/−), but no induction in the Ahr (−/−) (Fig. 2B). There was a significant basal expression of Cyp1b1 in the liver of all genotypes, and this expression was independent of the BP exposure. Constitutive Cyp1a1 expression level showed an Ahr gene–dose relationship in both the liver and lung, where Ahr (+/+) > Ahr (+/−) > Ahr (−/−) (Fig. 3). This was not observed for Cyp1b1.

HPLC-fluorescence analysis of the BP-protein adduct hydrolysis showed that the total BP-tetrol levels (the sum of the BP-tetrol I, BP-tetrol II and BP-tetrol III) were significantly higher in the Ahr (−/−) group compared to Ahr (+/+) and Ahr (+/−), in all of the tissues (Fig. 4; Table 1). In general, the total levels of BP-tetrols were,
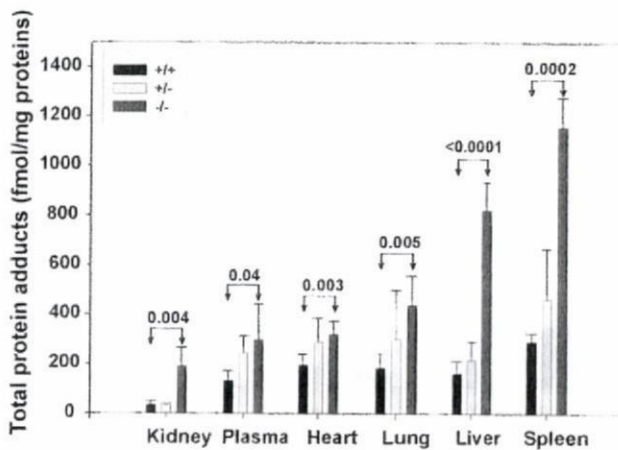

Fig. 4. Total sum (fmol/mg proteins) of the protein adduct hydrolysis products in kidney, plasma, heart, lung, liver and spleen from BP exposed mice. The tetrols were measured by HPLC-fluorescence as described in Section 2. The values are the sum of the BP-tetrol I, BP-tetrol II and BP-tetrol III. The BP-tetrol values are the means ± S.D. of data from six animals of each genotype. Means were compared by the independent samples t-test with Welch correction.

in descending order, spleen, liver, lung, heart, plasma and kidney. When examining specific tetrol levels, the BP-tetrol-I-1 and BP-tetrol-II-2 showed an inverse relationship compared to the Ahr gene–dose, with Ahr (−/−) > Ahr (+/−) > Ahr (+/+). In liver an increased ratio of BP-tetrol-II-2 to BP-tetrol-I-1 was found in Ahr (−/−) mice. There were significantly higher levels of the BP-tetrol I-1 and BP-tetrol II-2 in all the tissues in Ahr (−/−) group compared to the wild type animals (Fig. 5). In liver, BP-DNA adducts were found to parallel the levels of BP-protein adducts (Fig. 6).

The levels of unbound BP-tetrols were substantially higher in the Ahr (−/−) mice (Table 2). The lung and spleen displayed the highest levels while the heart and liver contained the lowest levels of free metabolites. The levels of unmetabolized BP were also significantly higher in the Ahr (−/−) mice as compared to the wild type mice. The Ahr (−/−) mice showed the highest levels of BP in the distal organs like lung and spleen, and the lowest levels in the liver. The BP content was 300 times higher in Ahr (−/−) lung and 190 times higher in Ahr (−/−) spleen compared to the corresponding levels in lung and spleen in the Ahr (+/+) (Table 2).

The formation of sulphate and glucoronide conjugates in the lung, spleen and heart were significantly higher in the Ahr (−/−) as compared to the Ahr (+/+). The highest levels of conjugates were found in kidney in both Ahr (−/−) and Ahr (+/+). The conjugate levels in kidney were higher in the Ahr (−/−) as compared to Ahr (+/+), but the difference was not statistically significant. Unconjugated phenolic compounds were detected in kidney and liver in both Ahr (+/+) and Ahr (−/−) mice, although Ahr (−/−) mice displayed the highest levels. These compounds were otherwise not found in the other organs (Table 2).

Table 1
BP-tetrol levels in internal organs and plasma from Ahr (+/+) and Ahr (−/−) mice

	Ahr (+/+)				Ahr (−/−)			
	BP-tetrol I	BP-tetrol II	BP-tetrol III	Sum	BP-tetrol I	BP-tetrol II	BP-tetrol III	Sum
Kidney	25.6 ± 4.9	7.7 ± 2.3	5.9 ± 1.9	39.2 ± 8.4	127.6 ± 59.2	42.4 ± 11.5	19.4 ± 6.3	$189.4 \pm 73.3^*$
Plasma	40.4 ± 12.9	48.0 ± 14.2	42.2 ± 13.2	130.6 ± 39.5	113.7 ± 55.2	116.4 ± 60.0	63.9 ± 32.0	294.0 ± 145.4
Heart	89.9 ± 19.3	63.7 ± 16.5	40.3 ± 9.3	194.0 ± 43.6	178.7 ± 29.0	97.2 ± 19.9	42.0 ± 6.3	$317.9 \pm 54.1^*$
Lung	107.9 ± 33.4	48.7 ± 18.4	25.1 ± 9.1	181.7 ± 59.7	258.4 ± 70.0	134.7 ± 40.4	41.8 ± 10.4	$434.9 \pm 118.8^*$
Liver	84.2 ± 24.6	47.1 ± 19.3	27.9 ± 11.0	159.3 ± 50.4	261.8 ± 41.0	471.1 ± 79.5	87.1 ± 19.1	$819.9 \pm 112.7^*$
Spleen	194.0 ± 26.2	64.3 ± 9.4	30.6 ± 4.8	289.0 ± 34.9	737.2 ± 122.3	287.4 ± 22.7	131.4 ± 15.2	$1156.0 \pm 134.8^*$

BP-tetrol levels (fmol/mg proteins) from the protein adduct hydrolysis expressed as the means $\pm$ S.D. of data from six individual animals in Ahr (+/+) vs. Ahr (−/−) mice.

* Statistically significant difference between Ahr (+/+) and Ahr (−/−) mice at $p < 0.05$ (independent samples t-test with Welch correction).
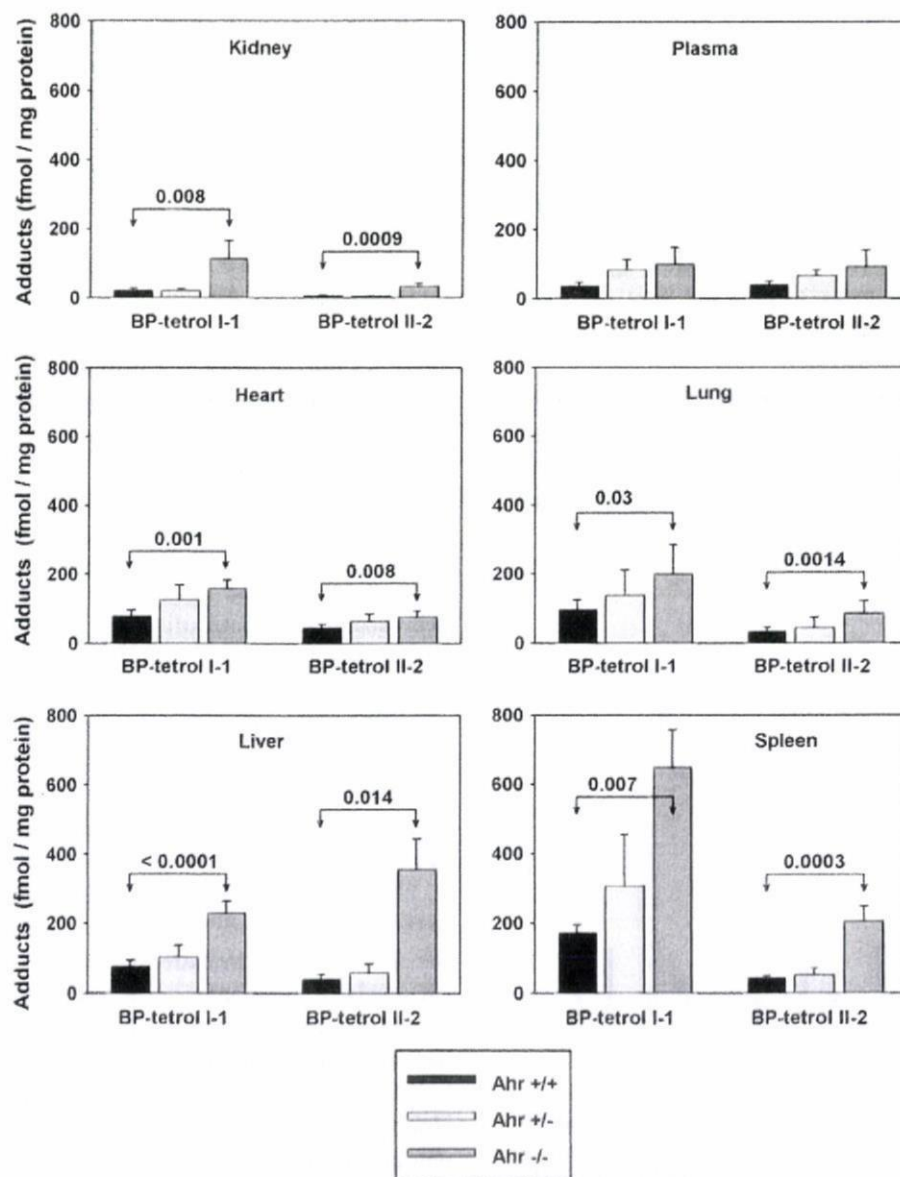

Fig. 5. The BP-tetrol I-1 and BP-tetrol II-2 in kidney, plasma, heart, lung, liver and spleen. In all cases, the tetrol levels are significantly higher in the Ahr (−/−) as compared to the Ahr (+/+). Means were compared by the independent samples t-test with Welch correction.
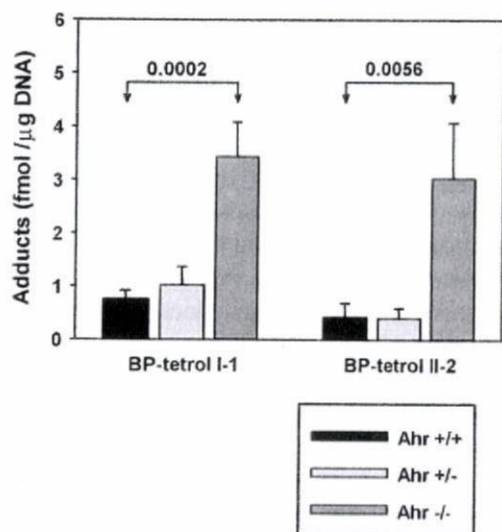
Fig. 6. BP-tetrol I-1 and BP-tetrol II-2 measured after hydrolysis of DNA-adducts in liver of BP exposed mice. Levels of both tetrols were significantly higher in Ahr (−/−) compared to Ahr (+/+). Means were compared by the independent samples t-test with Welch correction ($p < 0.05$).

4. Discussion

In the present study, the metabolism of BP given by gavage in Ahr knockout, heterozygotes and wild type mice has been compared. A significant accumulation of unmetabolized BP and increased levels of adducts and metabolites were found in Ahr (−/−) as compared to Ahr (+/−) and Ahr (+/+) mice. The BP-tetrol levels showed an inverse relationship compared to the Ahr gene–dose. In the liver of the Ahr (−/−) mice, the levels of BP-tetrol II-2 were higher than BP-tetrol I-1. These results indicate that the Ahr (−/−) mice have a higher formation of the less carcinogenic BPDE II than of the ultimate carcinogenic BPDE I in the liver. However, this pattern was not observed in the other tissues. The use of tetrols as surrogate markers for protein adducts is a highly specific and valuable biomarker method (Jansen et al., 1994; Rahn et al., 1982). Although less sensitive, the HPLC-fluorescence method gives valuable structural information regarding the formation of diolepoxides in the BP metabolism compared to ^{32}P-postlabeling (Eriksson et al., 2004).

The gastrointestinal tract and the liver are important in detoxicating orally administrated BP (Nebert, 1989). In the present study, organs distal to the stomach (the site of administration) like lung and spleen from Ahr (−/−) mice showed the highest levels of unmetabolized BP as compared to the other organs in Ahr (−/−) mice, and to the lung and spleen in the Ahr (+/+) and Ahr (+/−) mice.

Table 2
BP metabolite levels in internal organs and plasma from Ahr (+/+) and Ahr (−/−) mice

	Ahr (+/+)					Ahr (−/−)				
	BP	Protein adducts	Free tetrols	Diols/phenols	Conjuagtes	BP	Protein adducts	Free tetrols	Diols/phenols	Conjugates
Lung	175 ± 115	182 ± 60	26 ± 10	ND	150 ± 49	56306 ± 14724*	435 ± 119*	1219 ± 235*	ND	1754 ± 1522*
Spleen	219 ± 130	289 ± 35	15 ± 2	ND	59 ± 28	41085 ± 27678*	1156 ± 135*	1055 ± 132*	ND	1230 ± 657*
Plasma	580 ± 161	131 ± 39	–	–	–	20620 ± 10667*	294 ± 145	–	–	–
Heart	162 ± 144	194 ± 44	6 ± 3	ND	53 ± 12	17272 ± 9325*	318 ± 54*	573 ± 109*	ND	507 ± 294*
Kidney	833 ± 542	39 ± 8	25 ± 12	158 ± 92	15222 ± 5319	14278 ± 2364*	189 ± 73*	857 ± 280*	2650 ± 627	20606 ± 4167
Liver	65 ± 46	159 ± 50	20 ± 9.1	93 ± 70	1341 ± 355	8070 ± 5558*	820 ± 113*	695 ± 295*	1912 ± 591	6479 ± 3392*

Metabolites (fmol/mg proteins) expressed as the means ± S.D. of data from six individual animals in Ahr (+/+) vs. Ahr (−/−) mice.
* Statistically significant difference between Ahr (+/+) and Ahr (−/−) mice at $p < 0.05$ (independent samples t-test with Welch correction); ND, not detected; –, not measured.

The higher levels of BP in the Ahr (−/−) mice may be explained by reduced metabolism in the liver and therefore less presystemic elimination through the gut. This has also been observed with Ah non-responsive mice that were orally exposed to BP. The systemic exposure to BP increased in organs distal to the site of administration, as spleen and bone marrow, resulting in higher toxicity of BP and increased cell turnover (Galvan et al., 2003; Nebert, 1989). The high levels of adducts, metabolites and BP found in our Ahr (−/−) mice should then induce a higher genotoxic effect in the knockout as compared to the wild type.

Recently, it was found that deletion of the Cyp1a1 and Cyp1a1/1b1 genes resulted in a slow clearance of BP and increased DNA adducts in liver, spleen and bone marrow as measured by ^{32}P-postlabeling (Uno et al., 2004, 2006). In these studies, the mice received an oral dose of 125 mg/kg/day of BP continuously. The higher adduct levels were explained by a reduced phase II conjugation due to a loser coupling between the metabolizing enzymes in the knockout mice and the phase II conjugating enzymes, indicating that the induction of Cyp1a1 was protective and more important in the detoxification than the bioactivation of BP. Meanwhile, Cyp1b1 was suggested to be more important in the bioactivation of BP leading to adduct formation in spleen and bone marrow, and damage to the immune system (Uno et al., 2004, 2006).

In the present study, the basal expression of Cyp1a1 in lung and liver were almost not detectable, but highly induced in the wild type mouse. In contrast, basal expression of Cyp1b1 was present in lung and liver of all genotypes. In the Ahr (+/+) mice, the Cyp1b1 was induced in the lung, but in the liver. We have not found any sign of induction of Cyp1a1/1b1 in the Ahr (−/−) mice. Nevertheless, the BP metabolism in our study could partly be explained by constitutive expression of Cyp1b1. The BP metabolism observed in the Ahr (−/−) may also be evidence of an Ahr independent bioactivation and biotransformation of BP (Kondraganti et al., 2003). There are other Cyp isoforms (Cyp1a2, Cyp2–Cyp4) that may be involved (Shou et al., 1994), together with other oxidative enzymes. Kondraganti et al. (2003) found that an i.p. dose of BP induced formation of equal amounts of hepatic BP-DNA adducts in both Ahr (+/+) and Ahr (−/−) mice. Although BP did not induce Cyp1a1/1a2 in Ahr (−/−), they measured basal expression of Cyp1a1/1b1 in both Ahr (+/+) and Ahr (−/−) liver. Based on these results they proposed the existence of Ahr independent bioactivation of BP in the knockout mice. There are also reports of Ahr independent induction of Cyp1a1/1a2 and Cyp1b1 (Delescluse et al., 2000;

Galvan et al., 2005; Nakatsuru et al., 2004), that may depend on the type of PAH and the administration route. Nakatsuru et al. (2004) found that dibenzo[a,l]pyrene (DB[a,l]P), after skin application, induced low levels of Cyp1a1 in the Ahr (−/−) mouse skin, while BP and 7,12-dimethylbenz[a]anthracene (DMBA) was not found to induce any Cyp1a1. Galvan et al. observed Ahr independent bioactivation of BP and DMBA in bone marrow in Ahr non-responsive mice. The mice were given an i.p. dose of BP, which apparently increased the systemic exposure and toxicity of BP (Galvan et al., 2005). Finally, data from Cyp knockout studies could also support the idea of an Ahr independent bioactivation of BP (Uno et al., 2004, 2006).

There appears to be an active phase II conjugation in the Ahr (−/−) due to the formation of conjugates in all the tissues examined. This could be the result of a basal expression of phase II enzymes or an Ahr independent phase II induction. At the same time, the higher levels of adducts and free tetrols found in the Ahr (−/−) points towards a reduced phase II conjugation (Nebert et al., 2004). The higher levels of conjugates in the Ahr (−/−) might also be the effect of a reduced transport of water soluble compounds out of the cell, rather than an increased formation of conjugates (Ebert et al., 2005). Thus, in the absence of a functional Ahr receptor, and a proper induction of the phases I and II, and probably phase III enzymes (Klaassen, 2002; Xu et al., 2005), there appears to be a lower metabolic clearance of BP resulting in increased levels of DNA and protein adducts, metabolites and conjugates in the Ahr (−/−) mice.

The Ahr (−/−) mice have been found to be protected against BP induced carcinogenicity in the skin. On the other hand, there are reports indicating that the Ahr (−/−) mice may not be less susceptible to BP induced adduct formation (Kondraganti et al., 2003). In addition, toxicity of BP increases in Ahr non-responsive mice (Galvan et al., 2003; Galvan et al., 2005; Nebert, 1989) and Cyp knockout mice (Uno et al., 2004, 2006).

In conclusion, increased levels of protein and DNA adducts, metabolites and unmetabolized BP in mice lacking the Ahr were observed after oral exposure to BP. This may partly be explained by an Ahr independent and/or delayed bioactivation of BP in the Ahr knockout mice. The DNA-adduct level resulting from exposure to PAH has been suggested to represent not only a molecular exposure marker, but also a marker of cancer risk. Further studies are needed to clarify the persistence of BP adducts in Ahr (−/−) after oral exposure and their relation to cancer.

Acknowledgements

References

Beach, A.C., Gupta, R.C., 1992. Human biomonitoring and the ^{32}P-postlabelling assay. Carcinogenesis 13, 1053–1074.

Berge, G., Ovrebo, S., Eilertsen, E., Haugen, A., Mollerup, S., 2004. Analysis of resveratrol as a lung cancer chemopreventive agent in A/J mice exposed to benzo[a]pyrene. Br. J. Cancer 91, 1380–1383.

Conney, A.H., 1982. Induction of microsomal enzymes by foreign chemicals and carcinogenesis by polycyclic aromatic hydrocarbons: G.H.A. Clowes Memorial Lecture. Cancer Res. 42, 4875–4917.

Delescluse, C., Lemaire, G., de, S.G., Rahmani, R., 2000. Is CYP1A1 induction always related to AHR signaling pathway? Toxicology 153, 73–82.

Dipple, A., 1995. DNA adducts of chemical carcinogens. Carcinogenesis 16, 437–441.

Ebert, B., Seidel, A., Lampen, A., 2005. Identification of BCRP as transporter of benzo[a]pyrene conjugates metabolically formed in Caco-2 cells and its induction by Ah-receptor agonists. Carcinogenesis 26, 1754–1763.

Eriksson, H.L., Zeisig, M., Ekstrom, L.G., Moller, L., 2004. 32P-postlabeling of DNA adducts arising from complex mixtures: HPLC versus TLC separation applied to adducts from petroleum products. Arch. Toxicol. 78, 174–181.

Galvan, N., Jaskula-Sztul, R., MacWilliams, P.S., Czuprynski, C.J., Jefcoate, C.R., 2003. Bone marrow cytotoxicity of benzo[a]pyrene is dependent on CYP1B1 but is diminished by Ah receptor-mediated induction of CYP1A1 in liver. Toxicol. Appl. Pharmacol. 193, 84–96.

Galvan, N., Teske, D.E., Zhou, G., Moorthy, B., MacWilliams, P.S., Czuprynski, C.J., Jefcoate, C.R., 2005. Induction of CYP1A1 and CYP1B1 in liver and lung by benzo(a)pyrene and 7, 12-d imethylbenz(a)anthracene do not affect distribution of polycyclic hydrocarbons to target tissue: role of AhR and CYP1B1 in bone marrow cytotoxicity. Toxicol. Appl. Pharmacol. 202, 244–257.

Harvey, R.G., Geacintov, N.E., 1988. Intercalation and binding of carcinogenic hydrocarbon metabolites to nucleic acids. Acc. Chem. Res. 21, 66–73.

Hogan, M.E., Dattagupta, N., Whitlock Jr., J.P., 1981. Carcinogen-induced alteration of DNA structure. J. Biol. Chem. 256, 4504–4513.

IARC Monographs, 1983a. IARC Monographs on the Evaluation of the Carciongenic Risk of Chemical to Humans, Chemical, Environmental and Experimental Data, vol. 32, Part 1. International Agency for Research on Cancer, Lyon, France.

IARC Monographs, 1983b. IARC Monographs on the Evaluation of the Carciongenic Risk of Chemical to Humans, Industrial Exposures in Aluminium Production, Coal Gasification, Coke and Iron and Steel Founding, vol. 34, Part 3. International Agency for Research on Cancer, Lyon, France.

Jansen, E.H.J.M., van den Berg, R.H., Dinant Kroese, E., 1994. Liquid chromatographic analysis and stability of benzo[a]pyrene-tetrols in blood protein adducts in rats after exposure to benzo[a]pyrene. Anal. Chim. Acta 290, 86–93.

Klaassen, C.D., 2002. Xenobiotic transporters: another protective mechanism for chemicals. Int. J. Toxicol. 21, 7–12.

Kondraganti, S.R., Fernandez-Salguero, P., Gonzalez, F.J., Ramos, K.S., Jiang, W., Moorthy, B., 2003. Polycyclic aromatic hydrocarbon-inducible DNA adducts: evidence by 32P-postlabeling and use of knockout mice for Ah receptor-independent mechanisms of metabolic activation in vivo. Int. J. Cancer 103, 5–11.

Lowry, O.H., Rosebrough, N.J., Farr, A.L., Randall, R.J., 1951. Protein measurement with the folin phenol reagent. J. Biol. Chem. 193, 265–275.

McFadyen, M.C., Rooney, P.H., Melvin, W.T., Murray, G.I., 2003. Quantitative analysis of the Ah receptor/cytochrome P450 CYP1B1/CYP1A1 signalling pathway. Biochem. Pharmacol. 65, 1663–1674.

Nakatsuru, Y., Wakabayashi, K., Fujii-Kuriyama, Y., Ishikawa, T., Kusama, K., Ide, F., 2004. Dibenzo[A,L]pyrene-induced genotoxic and carcinogenic responses are dramatically suppressed in aryl hydrocarbon receptor-deficient mice. Int. J. Cancer 112, 179–183.

Nebert, D.W., 1989. The Ah locus: genetic differences in toxicity, cancer, mutation, and birth defects. Crit. Rev. Toxicol. 20, 153–174.

Nebert, D.W., Dalton, T.P., Okey, A.B., Gonzalez, F.J., 2004. Role of aryl hydrocarbon receptor-mediated induction of the CYP1 enzymes in environmental toxicity and cancer. J. Biol. Chem. 279, 23847–23850.

Nebert, D.W., Roe, A.L., Dieter, M.Z., Solis, W.A., Yang, Y., Dalton, T.P., 2000. Role of the aromatic hydrocarbon receptor and [Ah] gene battery in the oxidative stress response, cell cycle control, and apoptosis. Biochem. Pharmacol. 59, 65–85.

Rahn, R.O., Chang, S.S., Holland, J.M., Shugart, L.R., 1982. A fluorometric-HPLC assay for quantitating the binding of benzo[a]pyrene metabolites to DNA. Biochem. Biophys. Res. Commun. 109, 262–268.

Sagredo, C., Olsen, R., Greibrokk, T., Molander, P., Ovrebo, S., 2006. Epimerization and stability of two new cis-benzo[a]pyrene tetrols by the use of liquid chromatography-fluorescence and mass spectrometry. Chem. Res. Toxicol. 19, 392–398.

Shimizu, Y., Nakatsuru, Y., Ichinose, M., Takahashi, Y., Kume, H., Mimura, J., Fujii-Kuriyama, Y., Ishikawa, T., 2000. Benzo[a]pyrene carcinogenicity is lost in mice lacking the aryl hydrocarbon receptor. Proc. Natl. Acad. Sci. U.S.A. 97, 779–782.

Shou, M., Korzekwa, K.R., Crespi, C.L., Gonzalez, F.J., Gelboin, H.V., 1994. The role of 12 cDNA-expressed human, rodent, and rabbit cytochromes P450 in the metabolism of benzo[a]pyrene and benzo[a]pyrene trans-7,8-dihydrodiol. Mol. Carcinog. 10, 159–168.

Stowers, S.J., Anderson, M.W., 1985. Formation and persistence of benzo(a)pyrene metabolite-DNA adducts. Environ. Health Perspect. 62, 31–39.

Uno, S., Dalton, T.P., Derkenne, S., Curran, C.P., Miller, M.L., Shertzer, H.G., Nebert, D.W., 2004. Oral exposure to benzo[a]pyrene in the mouse: detoxication by inducible cytochrome P450 is more important than metabolic activation. Mol. Pharmacol. 65, 1225–1237.

Uno, S., Dalton, T.P., Dragin, N., Curran, C.P., Derkenne, S., Miller, M.L., Shertzer, H.G., Gonzalez, F.J., Nebert, D.W., 2006. Oral benzo[a]pyrene in Cyp1 knockout mouse lines: CYP1A1 important in detoxication, CYP1B1 metabolism required for immune

damage independent of total-body burden and clearance rate. Mol. Pharmacol. 69, 1103–1114.

Veglia, F., Matullo, G., Vineis, P., 2003. Bulky DNA adducts and risk of cancer: a meta-analysis. Cancer Epidemiol. Biomarkers Prev. 12, 157–160.

Whitlock Jr., J.P., 1999. Induction of cytochrome P4501A1. Annu. Rev. Pharmacol. Toxicol. 39, 103–125.

Xu, C., Li, C.Y., Kong, A.N., 2005. Induction of phase I, II and III drug metabolism/transport by xenobiotics. Arch. Pharm. Res. 28, 249–268.

Unique and Overlapping Transcriptional Roles of Arylhydrocarbon Receptor Nuclear Translocator (Arnt) and Arnt2 in Xenobiotic and Hypoxic Responses[*]

Hiroki Sekine[‡], Junsei Mimura[‡§], Masayuki Yamamoto[‡], and Yoshiaki Fujii-Kuriyama[‡§1]

From the [‡]Center for Tsukuba Advanced Research Alliance and Institute of Basic Medical Sciences, University of Tsukuba, 1-1-1 Tennoudai, Tsukuba 305-8577, Japan and [§]SORST, Japan Science and Technology Agency, 4-1-8 Honcho, Kawaguchi, 332-0012 Japan

Arnt and the homologous Arnt2 share a high degree of sequence similarity and are believed to function as obligate common partners for a number of basic helix-loop-helix (bHLH)-PAS transcription factors including arylhydrocarbon receptor (AhR) and HIFα. Genetic disruption of both Arnt and Arnt2 demonstrated both unique and overlapping functions in response to environmental stimuli and during mouse development. Either stably or transiently expressed Arnt/Arnt2 wild type and various mutants or chimeric constructs in Hepa1-c4 cells exhibit similar levels of hypoxic response element-driven reporter gene expression and the induction of endogenous *Glut-1* through binding with HIFα in response to hypoxia. In contrast, we observed clear functional differences in the ability of Arnt and Arnt2 to induce xenobiotic response element-driven reporter and endogenous *CYP1A1* gene expression. In contrast with Arnt, Arnt2 was practically incapable of interacting with ligand-activated AhR to induce the expression of target genes for xenobiotic-metabolizing enzymes in response to xenobiotics. The differential binding of AhR by Arnt and Arnt2 can be ascribed to a single His/Pro amino acid difference in the PASB region of Arnt and Arnt2, suggesting that the PASB/PASB interaction between bHLH-PAS transcription factors plays a selective role for their specific partner molecule.

Arylhydrocarbon receptor nuclear translocator (Arnt)[2] is a nuclear localized transcription factor that is a canonical member of a transcription factor family consisting of an N-terminal basic helix-loop-helix (bHLH) domain followed by a PAS domain, so named because it is conserved among Per, Arnt, and Sim (1–5). In contrast, the arylhydrocarbon receptor (AhR), a member of the same transcription factor family, associates with an HSP90 complex in the cytoplasm and, upon binding an exogenous inducer such as 3-methylcholanthrene (3MC) or 2,3,7,8-tetrachlorodibenzo-*p*-dioxin (TCDD), translocates from the cytoplasm to the nucleus. Within the nucleus, AhR dissociates from HSP90 and forms a heterodimer with Arnt. The newly formed AhR·Arnt complex binds *cis*-acting DNA enhancer sequences, known as xenobiotic response element (XRE), or dioxin response element (DRE), to enhance the expression of a number of drug-metabolizing enzyme genes including cytochrome P4501A1 (*CYP1A1*) (6). Furthermore, AhR·Arnt signaling is essential for liver and palate development as well as normal reproductive homeostasis, as shown by studies on AhR-deficient mice (7, 8).

Under normoxic conditions, expression of the bHLH-PAS transcription factors hypoxia-inducible factor (HIF)-1α and HIF2α is negatively regulated by the von Hippel-Lindau tumor suppressor protein through the 26 S proteasome (9). However, under hypoxic conditions, HIFα is stabilized and translocates into the nucleus, where it forms a heterodimer with Arnt and binds the hypoxic response element (HRE) leading to the expression of target genes involved in glycolysis, erythropoiesis, and angiogenesis (6). In addition, HIF1α and HIF2α may be involved in normal embryonic development (10–12).

Arnt2, first identified as a homologue with a high degree of sequence similarity to Arnt, undergoes heterodimerization with other bHLH-PAS transcription factors, but unlike the ubiquitously expressed Arnt, Arnt2 expression is restricted to neural tissues and the kidney (13, 14). Arnt2-deficient mice die in the perinatal period and have impaired hypothalamic development (15), but targeted disruption of the Arnt gene leads to embryonic lethality between E9.5 and E10.5 characterized by disrupted placental, hematopoietic and yolk sac vascular development (16–19). When compound heterozygous Arnt$^{2+/-}$ and Arnt$^{+/-}$ mice were mated, all homozygous double mutant mice died before E8.5, and a much smaller number of compound heterozygous Arnt$^{-/-}$Arnt$^{2+/-}$ or Arnt$^{+/-}$ Arnt2$^{-/-}$ mutant fetuses were found to be alive at E8.5 than expected from Mendelian genetics, suggesting a strong genetic interaction between Arnt2 and Arnt during mouse development (20). Thus, although the expression and functions of Arnt2 and Arnt are not entirely overlapping, there is a strong genetic and functional interaction during development. We wished to deter-

---

[1] To whom correspondence should be addressed: Center for Tsukuba Advanced Research Alliance, University of Tsukuba, 1-1-1 Tennoudai, Tsukuba, Ibaraki 305-8577 Japan. Tel.: 81-29-853-7323; Fax: 81-29-853-7318; E-mail: ykfujii@tara.tsukuba.ac.jp.

[2] The abbreviations used are: Arnt, arylhydrocarbon receptor nuclear translocator; mArnt, mouse Arnt; 3MC, 3-methylcholanthrene; TCDD, 2,3,7,8-tetrachlorodibenzo-*p*-dioxin; bHLH, basic helix-loop-helix; AhR, arylhydrocarbon receptor; HIF, hypoxia-inducible factor; XRE, xenobiotic response element; HRE, hypoxic response element; E, embryonic day; PBS, phosphate-buffered saline; WT, wild type; aa, amino acid(s).

-899-

mine the biochemical and molecular basis for the observed differential roles of Arnt and Arnt2 in physiology and development. Although in our previous report on the transient DNA transfection experiments Arnt2 exhibited some 20% transactivation activity of Arnt with XRE-driven reporter gene (13), stably expressed Arnt2 in transformant cells failed to induce the expression of the XRE-reporter and endogenous *CYP1A1* genes in sharp contrast with studies of Arnt. Interestingly, the differential activity between Arnt and Arnt2 in heterodimer formation with AhR can be ascribed to a single amino acid replacement in the PASB domain.

EXPERIMENTAL PROCEDURES

Plasmids—mArnt and mArnt2 in pBSK were cleaved with NcoI and fused at their N termini with a 3xFLAG tag derived from p3xFLAG-CMV-10 (Sigma). pBSK3xFLAG-Arnt and pBSK3xFLAG-Anrt2 were cleaved with EcoRI and XbaI, and the isolated inserts were blunt-ended and subsequently cloned into XbaI-digested blunt-ended pEFBOS (21) to produce pBOS3xFLAG-Arnt and pBOS3xFLAG-Arnt2. Arnt/Arnt2 chimeras were produced and designated as follows: 3xFLAG-A1(A2TA); 3xFLAG-Arnt N-terminal region (aa 1–465) was connected with the Arnt2 C-terminal region (aa 440–712), 3xFLAG-A2(A1TA); 3xFLAG-Arnt2 N-terminal region (aa 1–439) was connected with the Arnt C-terminal region (aa 466–791), 3xFLAG-A1(A2AB), and 3xFLAG-A2(A1AB); 3xFLAG Arnt or Arnt2 PAS domain was replaced with the Arnt2 or Arnt PAS domain (Arnt-(156–465), Arnt2-(130–439)), respectively (see Fig. 2*A* for summary), 3xFLAG-A1(A2A); 3xFLAG-Arnt PASA domain was replaced with the Arnt2 PASA domain (Arnt-(156–356), Arnt2-(130–330)), respectively (see Fig. 5*A* for summary), 3xFLAG-A1(A2B); 3xFLAG Arnt PASB domain was replaced with the Arnt2 PASB domain (Arnt-(357–465), Arnt2-(331–439)) (see Fig. 5*A* for summary). These cDNA expression vectors were generated using the standard methods and confirmed by sequencing, and the inserts were then cloned into the pBOS vector. pBOS3xFLAG-ArntH378P, pBOS3xFLAG-A1(A2A)H378P, and pBOS-3xFLAG-A1(A2B)P352H were generated by site-directed mutagenesis using the Sculptor *in vitro* mutagenesis system (Amersham Biosciences) with pBOS3xFLAG-Arnt, pBOS3xF-LAG-A1(A2A), and pBOS3xFLAG-A1(A2B), as templates, respectively (See Fig. 5*A* for summary).

For construction of pBOSGAL4DBD-Arnt-bHLHPAS-(91–465) and pBOSGAL4DBD-Arnt2-bHLHPAS-(65–439), mArnt-bHLHPAS and mArnt2-bHLHPAS region fragments were produced by PCR, using pBOS3xFLAG-Arnt and pBOS3xFLAG-Arnt2 as templates, and confirmed by sequencing. These fragments were cloned into the pBOSGAL4DBD vector (22). Chimeric constructs were produced and designated as follows: pBOSGAL4DBD-A1A2-bHLHPAS; pBOSGAL-4DBD-Arnt-bHLHPAS N-terminal region (aa 91–257) fused with the Arnt2-bHLHPAS C-terminal region (aa 232–439), pBOSGAL4DBD-A1A2A1-bHLHPAS, A1A1A2-bHLHPAS, A1A2A1-2-bHLHPAS, and A1A1A2-2-bHLHPAS. The sequences of the following regions (aa 258–333, 334–465, 334–397, and 398–465) from pBOSGAL4DBD-Arnt-bHLHPAS were exchanged, respectively, with the corresponding regions

of Arnt2-(232–307), -(308–439), -(308–371), and -(372–439). pBOSGAL4DBD-ArntH378P-bHLHPAS was generated by site-directed mutagenesis using pBOSGAL4DBD-Arnt-bHLHPAS as a template.

To produce pBOSVP16AD-mHIF1αΔC, the mHIF1αΔC-(1–613) fragment was generated by PCR using cDNA from Hepa1 RNA as a template and cloned into pGEM-T-Easy vector (Promega). After sequencing, the excised cDNA fragment was inserted into pBOSVP16AD multi-cloning sites (22).

Cell Culture—Hepa1-c4 (an Arnt-defective cell line of Hepa1c1c7 cells (23)), Hepa1, 293T, and HeLa cells were maintained, respectively, in high or low glucose Dulbecco's modified Eagle's medium (Sigma) supplemented with 10% fetal bovine serum (Sigma) and penicillin/streptomycin (Invitrogen) under 5.0% CO_2 at 37 °C.

Reporter Assay—All luciferase assays were performed using the Dual-Luciferase reporter assay system according to the manufacturer's protocol (Promega) with some modifications. Hepa1-c4 cells (2.0×10^4 cells/well) were plated in 24-well plates 24 h prior to transfection. Cells were co-transfected with pXRE4-SV40-Luc (22) or pHRE6-SV40-Luc reporter (24) using 1 ng of *Renilla* luciferase as an internal control and pBOS3xFLAG-Arnt, pBOS3xFLAG-Arnt2, or the chimeric constructs using FuGENE 6 transfection reagent (Roche Applied Science) according to the manufacturer's protocol. All cells were incubated for 24 h at 37 °C after transfection. pXRE4-SV40-Luc-transfected cells were treated with 1 μM 3MC, a potent inducer of XRE-driven transcription, or with Me_2SO and then incubated for an additional 18 h. To measure hypoxia-induced transcription, cells transfected with pHRE6-SV40-Luc were incubated under normoxic or hypoxic (1.0% O_2) conditions for an additional 16 h.

HeLa cells (2.5×10^4 cells/well) were cultured in 24-well plates for 24 h prior to transfection and then were cotransfected with pXRE4-SV40-Luc or pHRE6-SV40-Luc, 1 ng of *Renilla* luciferase as an internal control, effector plasmid (pBOS3x-FLAG-Arnt, pBOS3xFLAG-Arnt2, chimeric or mutant constructs), and partner molecule plasmid (either pBOSmAhR (22) or pBOShHif1α (24)) using Lipofectamine Plus (Invitrogen) according to the manufacturer's protocol. After an additional 24 h of incubation, cells were treated with 3MC or placed under hypoxic condition as described above.

For the Arnt-AhR two-hybrid assay, 293T cells (2.0×10^4 cells/well) were cultured in 24-well plates 24 h prior to transfection and cotransfected with 100 ng of pG3-Luc (22), 0.1 ng of *Renilla* luciferase reporter as an internal control, 10 ng of the bait plasmid (either pBOSGAL4DBD-Arnt, -Arnt2-bHLHPAS, or chimeric or mutant constructs), and 60 ng of prey plasmid (either pBOSVP16AD-mAhRΔC (22) or pBOSVP16AD-mAhRΔBΔC) using Lipofectamine Plus (Invitrogen). For Arnt-HIF1α two-hybrid assay, cultured 293T cells were cotransfected with 100 ng of pG3-Luc (22), 0.1 ng of *Renilla* luciferase reporter as an internal control, 2 ng of the bait plasmid (either pBOSGAL4DBD-mArnt, pBOSGAL4DBD-mArnt2-bHLHPAS, or chimeric and mutants constructs), and 5 ng of pBOSVP16AD-mHIF1αΔC as described above. 3MC and hypoxia treatment were performed as described above.
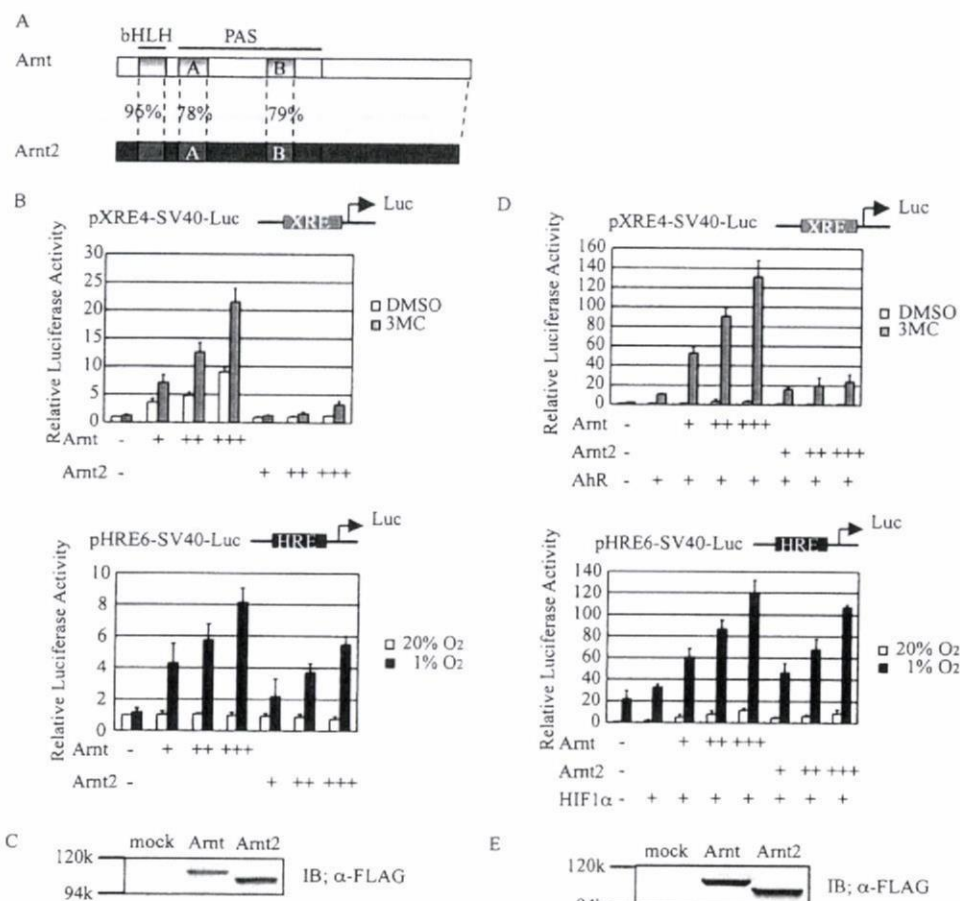
FIGURE 1. **Transcriptional activity of Arnt and Arnt2 on XRE- and HRE-driven reporter genes in Hepa1-c4 and HeLa cells.** *A*, amino acid identities between Arnt and Arnt2. *B*, transcriptional activity of Arnt and Arnt2 in Hepa1-c4 cells. Hepa1-c4 cells were transfected with 100 ng of pXRE4-SV40-Luc and increasing amounts (1, 10, and 100 ng) of 3xFLAG-Arnt or 3xFLAG-Arnt2 expression plasmids, incubated for 24 h, and treated with 1 μM 3MC or Me₂SO (dimethyl sulfoxide (*DMSO*)) for 18 h (*top panel*). For analysis of the hypoxic response, Hepa1-c4 cells were transfected with 100 ng of pHRE6-SV40-Luc and increasing amounts (1, 10, and 100 ng) of 3xFLAG-Arnt or 3xFLAG-Arnt2 expression plasmids. After 24 h of incubation, the cells were treated for 16 h under conditions of normoxia (20% O₂) or hypoxia (1% O₂) (*bottom panel*). The cell extracts were prepared from the treated cells and used for luciferase assays. Values are represented by mean ± S.D. of the results of three independent experiments normalized to *Renilla* luciferase activity used as an internal control. *C*, expression of Arnt and Arnt2 in Hepa1-c4 cells. Hepa1-c4 cells were transfected with 0.5 μg of the indicated expression construct in 6-well plates. The protein levels were evaluated by Western blotting using anti-FLAG antibody. Equal amounts of cell lysates were used for Western blot analysis. The *mock* lane represents cell lysate transfected with empty vector alone. *D*, transcriptional activity of Arnt and Arnt2 in HeLa cells. *Top panel*, XRE-driven reporter activity. HeLa cells were transfected with 10 ng of pXRE4-SV40-Luc, increasing amounts (0.1, 0.5, and 2 ng) of 3xFLAG-Arnt or -Arnt2 expression plasmids, and 10 ng of pBOSmAhR, and the reporter gene expression assays were performed as described in *B*. *Bottom panel*, HRE-driven reporter activity. HeLa cells were transfected with 10 ng of pHRE6-SV40-Luc, increasing amounts (0.1, 0.5, and 2 ng) of 3xFLAG-Arnt or -Arnt2 expression plasmids, and 20 ng of pBOShHIF1α, and the reporter gene expression assays were performed as described in *B*. Values are represented by mean ± S.D. of the results of three independent experiments normalized to *Renilla* luciferase activity used as an internal control. *E*, expression of Arnt and Arnt2 in HeLa cells. HeLa cells were transfected with 10 ng of the indicated expression construct in 6-well plates. *IB*, immunoblot.

AhR (Biomol), or anti-actin or anti-VP16AD (Santa Cruz Biotechnology) antibodies were used as primary reagents. After being washed three times in TBS (25 mM Tris/HCl (pH 7.5), 150 mM NaCl) containing 0.1% Triton X-100, membranes were incubated with species-specific horseradish peroxidase-conjugated secondary antibody (Zymed Laboratories Inc.). The protein-antibody complexes were visualized by the enhanced chemiluminescence detection system (Amersham Biosciences) according to the recommendations of the manufacturer.

Whole Cell Lysate Preparation for Coimmunoprecipitation—Hepa1-c4 cells stably transfected with pBOS-3xFLAG-Arnt, pBOS3xFLAG-Arnt2, or pBOS3xFLAG-ArntH-378P were incubated with 1 μM 3MC or Me₂SO for 2 h and washed with ice-cold phosphate-buffered saline followed by TBS. The cells were harvested by scraping, centrifuged at 5,000 rpm at 4 °C for 5 min, and suspended in TBS containing 1 mM CaCl₂, 1% Triton X-100, and protease inhibitor mixture (Roche Applied Science). The cells were vortexed and placed on ice for 5 min. The samples were then centrifuged at 15,000 rpm for 5 min at 4 °C, and the supernatants were reserved as whole cell lysates.

Coimmunoprecipitation Assay—The prepared whole cell lysate (200 μl) was added to 200 μl TBS with 1 mM CaCl₂ and protease inhibitor mixture and incubated with anti-FLAG antibody for 1 h at 4 °C. The reaction mixture was supplemented with 15 μl of protein A-agarose beads (Amersham Biosciences). After incubating for an additional 1 h at 4 °C, the beads were washed three times with TBS and resuspended in SDS sample buffer. The coimmunoprecipitated proteins were resolved by SDS-PAGE, and Western blot analysis was performed.

Immunohistochemistry—Hepa1-c4 cells stably transfected with pBOS3xFLAG-Arnt, pBOS3xFLAG-Arnt2, or pBOS3x-FLAG-ArntH378P were washed, fixed in 4% paraformaldehyde at room temperature for 10 min, and treated with cold acetone for 1 min on ice. After washing with PBS, the cells were incubated with 3% skim milk for 1 h at room temperature and treated with 10 μg/ml mouse anti-FLAG antibody for 16 h at 4 °C. After washing with PBS, the cells were subsequently

Generation of Stable Transformant Cell Lines—Hepa1-c4 cells were cotransfected with pSVneo and effector plasmid (either pBOS3xFLAG-Arnt, pBOS3xFLAG-Arnt2, or pBOS3x-FLAG-ArntH378P). After transfection, the cells were replated and incubated with selection medium containing 0.5 mg/ml Geneticin (Invitrogen).

Western Blot Analysis—Cells were dissolved in SDS sample buffer, and proteins were separated by SDS-PAGE for Western blot analysis. Proteins were then transferred to polyvinylidene difluoride membranes and blocked in 3% skim milk for 30 min. A rabbit anti-Arnt antiserum (25) or anti-FLAG (Sigma), anti-

-901-